Pergamon

PII: S0146-6380(97)00134-4

Org. Geochem. Vol. 28, No. 5, pp. 265–288, 1998

Printed in Great Britain
0146-6380/98 $19.00 + 0.00

Characterization of a highly resistant biomacromolecular material in the cell wall of a marine dinoflagellate resting cyst

JOHN P. KOKINOS*[1], TIMOTHY I. EGLINTON[2]†, MIGUEL A. GOÑI‡[2], JAAP J. BOON[3], PAMELA A. MARTOGLIO§[4] and DONALD M. ANDERSON[1]

[1]Department of Biology, Woods Hole Oceanographic Institution, Woods Hole, MA 02543, U.S.A., [2]Department of Marine Chemistry and Geochemistry, Woods Hole Oceanographic Institution, Woods Hole, MA 02543, U.S.A., [3]FOM Institute for Atomic and Molecular Physics, Unit for Mass Spectrometry of Macromolecular Systems, Kruislaan 407, 1098 SJ Amsterdam, The Netherlands and [4]Spectra-Tech Inc., 652 Glenbrook Road, Building 8, Stamford, CT 06906, U.S.A.

(Received 9 September 1997; returned to author for revision 6 November 1997; accepted 16 December 1997)

Abstract—The remarkable physical and chemical resistance of the organic cell walls enclosing resting cysts formed by several species of dinoflagellates has long invited questions regarding their composition. Traditionally, this resistance was thought to derive from the presence of "sporopollenin", a term originally coined to describe the highly refractory substance found in the walls of pollen and spores of higher plants. The lack of detailed chemical analyses of dinoflagellate materials, however, has left this practice open to question. Here we report the results of the first rigorous chemical characterization of resting cyst walls produced by a dinoflagellate, the extant marine species *Lingulodinium polyedrum* (formerly *Gonyaulax polyedra*). Resistant cell walls were isolated by sequentially treating cyst-producing laboratory cultures by solvent extraction, saponification, and acid hydrolysis. At each stage of processing, residues were characterized by light microscopy, FTIR microspectroscopy, elemental analysis, and direct ("in source") temperature–resolved mass spectrometry (DT–MS). Initial materials and final residues were further analyzed by Curie-point pyrolysis–gas chromatography–mass spectrometry (Py–GC/MS) and cupric oxide (CuO) oxidation. Overall, our results indicate an absence of extended *n*-hydrocarbon chains which typify aliphatic macromolecules ("algaenans") dominating the resistant fractions of other algae studied to date. In contrast the data suggest that the cell wall contains relatively condensed, predominantly aromatic structures, possibly cross-linked via carbon–carbon or ether bonds. The presence of prist-1-ene among the most prominent pyrolysis products also suggests that bound tocopherols function as additional structural elements in the wall material(s). The *L. polyedrum* resting cyst cell wall thus appears to contain a biomacromolecular substance that is distinct from both sporopollenin and aliphatic algaenans. These findings help to further establish a chemical basis for the preservation potential of organic biomacromolecules, and illuminate possible chemical/functional relationships among highly refractory substances from diverse biological sources.

Key words—dinoflagellates, resting cysts, biomacromolecules, sporopollenin, algaenans

INTRODUCTION

The dinoflagellates comprise a class of microscopic algae that is widely distributed in both marine and freshwater environments. As a group, these typically single-celled organisms show an extraordinary level of sophistication and diversity in form, structure, nutritional regime, habit, and life history (Spector, 1984; Taylor, 1987). Dinoflagellates are perhaps best known as biflagellated, free-swimming cells often abundant in the plankton where they play a key role in primary productivity and are the main cause of phenomena such as red tides and paralytic shellfish poisoning.

Like many other microorganisms, certain dinoflagellates have the ability to enter into a dormant or resting stage as part of their relatively complicated life cycle. These dormant stages, called resting cysts, often display morphologies radically different from those of the motile forms, and typically are characterized by a thick and highly specialized cell covering. For some dinoflagellate species, the resting cyst cell wall is composed of resistant materials that allow these structures to persist in the depositional environment long after germination of the cyst. The rich fossil record of the dinoflagellates, which extends back at least 225 million years, is in fact

*Hellenic College/Holy Cross, 50 Goddard Avenue, Brookline, Massachusetts 02146 U.S.A.
†To whom correspondence should be addressed.
‡Department of Geological Sciences, Earth and Water Sciences 302, University of South Carolina, Columbia, South Carolina 29208, U.S.A.
§Nicholet Instrument Corp., Suite M, 1355 Remington Road, Schaumburg, Illinois 60173 U.S.A.

composed almost exclusively of selectively preserved resting cyst cell walls (Evitt, 1961, 1985). In recent decades, fossil dinoflagellates have attracted considerable attention due primarily to their utility in biostratigraphic applications, particularly those relating to petroleum exploration (Williams and Bujak, 1985; Goodman, 1987).

Although a very small number of dinoflagellate fossils are calcareous or siliceous, most are non-mineral (i.e., organic) in composition. These latter forms are routinely isolated from consolidated sediment samples using standard palynological maceration techniques (digestion of rock minerals with concentrated HF and HCl; see Gray, 1965, and Barss and Williams, 1973), which typically leave the preserved cell walls morphologically unaltered. The remarkable physical and chemical resistance of these organic cell walls has long invited questions regarding their composition. Because fossil pollen and spores often co-occur with dinoflagellates in rock-extraction residues, it has become traditional among paleontologists and biologists (e.g., Eisenack, 1963; Atkinson *et al.*, 1972; Bujak and Davies, 1983; Evitt, 1985) to classify organic dinoflagellate fossil material under the general umbrella of "sporopollenin", a term originally coined to

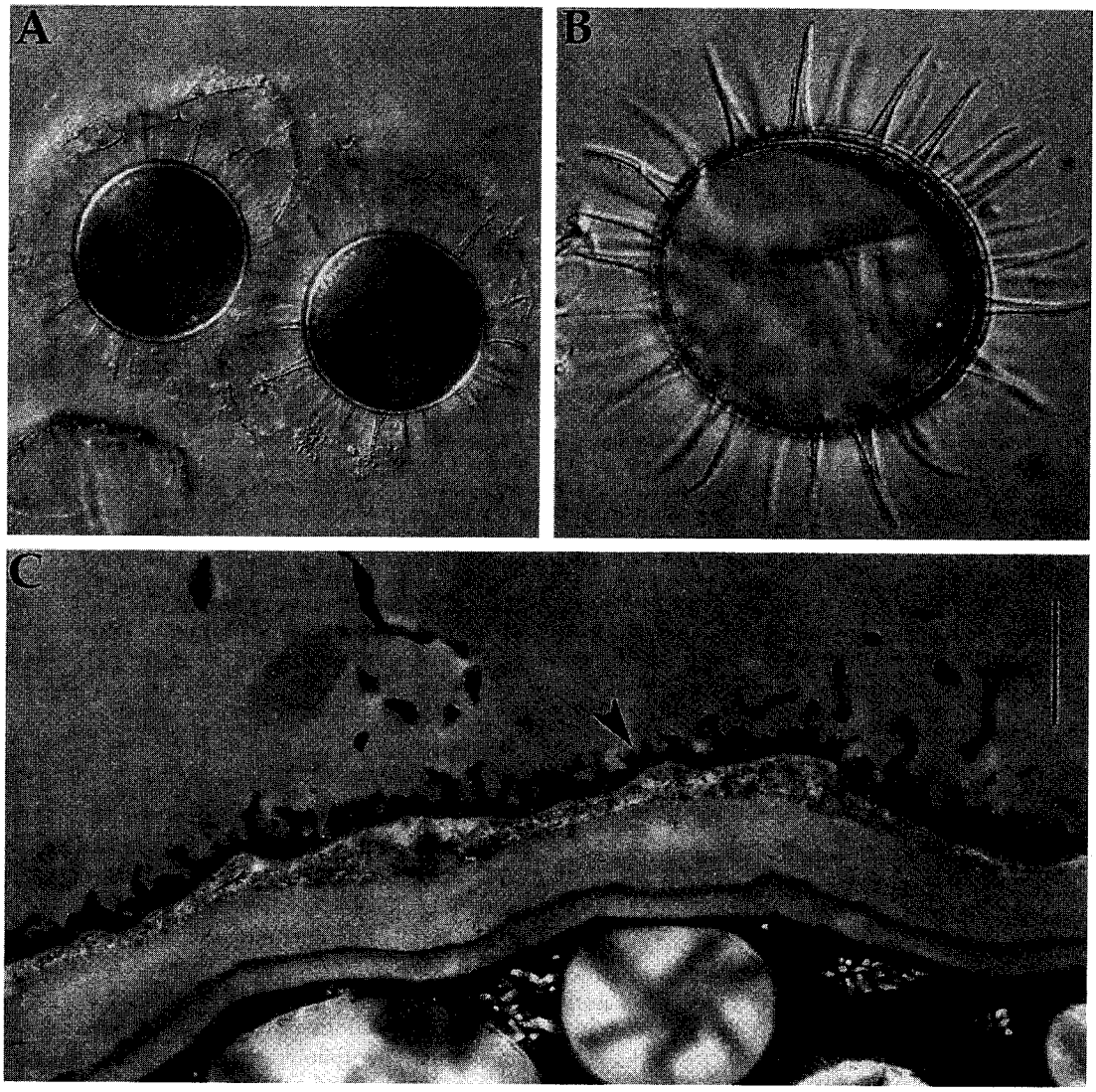

Fig. 1. Resting cysts of *Lingulodinium polyedrum*. Light photomicrographs (DIC) of: (a) Living specimens produced in laboratory cultures. Spherical central body ~50 μm in diameter; (b) Fossil *L. polyedrum* resting cyst recovered from Lower Miocene strata in France. In the paleontological literature, this morphotype is referred to as *L. machaerophorum*. (c) Transmission electron micrograph (TEM) of living resting cyst wall periphery. Scale bar ~1 μm. For TEM, living resting cysts were collected from culture vessels, fixed in a mixture of 2.5% glutaraldehyde and 2% para-formaldehyde, post-fixed in 1% osmium tetroxide, and en bloc stained with saturated uranyl acetate. Cells were then encapsulated in 2% agarose, dehydrated in a graded ethanol series, and embedded in Spurr resin. For further details of methodology and instrumentation see Kokinos (1994).

describe the highly refractory substance found in the pollen and spore walls (Zetsche and Vicari, 1931). The lack of detailed chemical analyses of dinoflagellate materials, however, has left this practice open to question.

In the present study, we report the results of the first rigorous chemical characterization of resting cyst walls produced by a dinoflagellate, the extant marine species *Lingulodinium polyedrum* (alias *Gonyaulax polyedra*). A typical *L. polyedrum* resting cyst, isolated either from coastal marine sediments or from cyst-producing laboratory cultures, consists of a spherical, cytoplasm-containing central body bearing numerous distinctive spines (Fig. 1(a)). Fossil representatives of this species (i.e., the preserved walls of the resting cyst, Fig. 1(b)) are commonly encountered in strata ranging in age from the Early Eocene (~54 million years ago) to the present (Williams *et al.*, 1993). Comparison of transmission electron microscopy (TEM) images of living *L. polyedrum* resting cyst walls (Fig. 1(c)) with those of fossil counterparts (Jux, 1971) shows the resistant material to be localized in the outermost wall layer and spines. These features are rapidly formed during resting cyst morphogenesis, and detailed observations of this process (Kokinos and Anderson, 1995) suggest a mechanism involving the self-assembly (polymerization) of precursor units. The biosynthetic, morphological and physiological characteristics of these resting cysts thus contrast sharply with those of the resistant biopolymers (algaenans) that are found in the cell walls of certain algae (e.g. Kadouri *et al.*, 1988). For our chemical investigations, a purified fraction of resistant cell wall components was obtained by sequentially treating culture-derived resting cysts by solvent extraction, saponification, and acid hydrolysis. The sample thus obtained was then characterized using a variety of optical, chemical, spectroscopic and pyrolytic techniques.

EXPERIMENTAL

Biological materials and culturing conditions

Laboratory cultures of *L. polyedrum* were established and maintained as described in Kokinos and Anderson (1995). Cultures were established in March 1990 using cysts isolated from sediments collected at Essvik Station 1 (water depth, 90 m), Gullmar Fjord, Sweden. Each strain was started from a single cyst. All dinoflagellate material utilized in the present study derived from a single strain (GpES-19). Although cultures were not axenic, examination under the microscope revealed any bacterial mass to be negligible. The majority of resting cyst production in batch cultures occurred during the 2 weeks following peak cell density (i.e., starting about 3.5–4 weeks after inoculation). After cyst production was complete, cultures tubes were stored under the same conditions used for actively growing cultures. To collect resting cyst material for analysis, cultures were harvested using a teflon policeman to gently scrape culture residue from tube bottoms. Loosened materials were transferred to centrifuge tubes, washed 5 times in Milli-Q water, briefly sonified, washed again 5 times, and then freeze-dried. One hundred culture tubes, each originally containing 20 ml of medium, yielded ~85 mg dry weight of initial material.

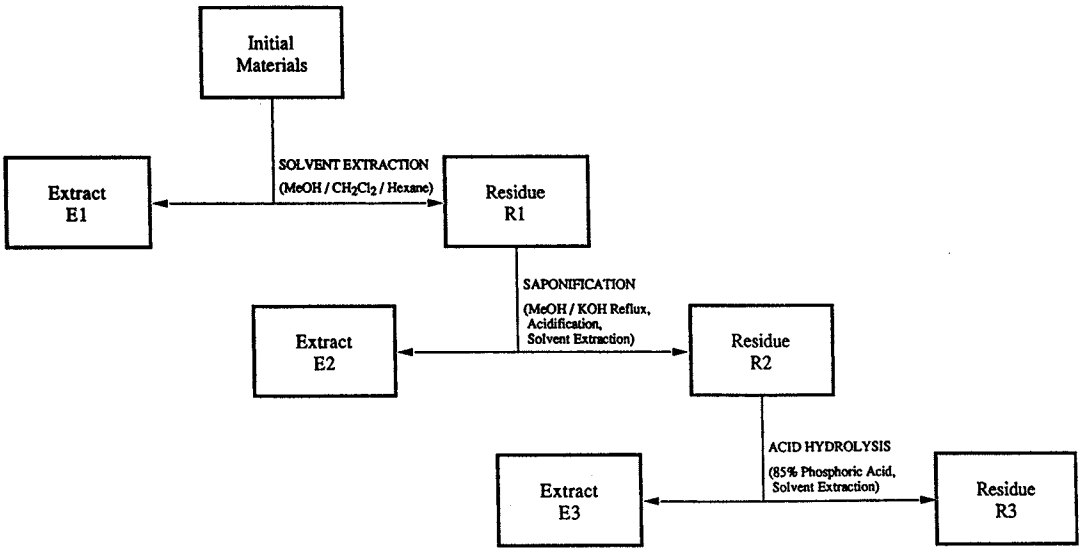

Fig. 2. Schematic illustration of procedures used to isolate resistant cell walls.

Isolation of resistant cell walls

Resting cyst cell walls were isolated using a 3-step procedure (solvent extraction, saponification, acid hydrolysis), shown schematically in Fig. 2.

Solvent extraction. The freeze dried culture sample was sequentially extracted ultrasonically at room temperature with a mixture of methanol (MeOH) and dichloromethane (CH_2Cl_2) (1/1, v/v, 2×) and CH_2Cl_2/hexane (4/1, v/v, 2×). After each extraction, the insoluble residue was recovered by centrifugation, ultimately yielding residue R1; extraction supernatants were combined and concentrated, resulting in extract E1.

Saponification. R1 was refluxed for 6 h in 6% KOH in MeOH/H_2O (9/1, v/v). After saponification, the reflux mixture was acidified to pH 4 by additions of 2 N HCl/MeOH (1/1, v/v). The residue was separated by centrifugation and the supernatant transferred to a separatory funnel. The residue was then ultrasonically extracted using H_2O (100%), MeOH/H_2O (1/1, v/v), MeOH (100%), MeOH/CH_2Cl_2 (1/1, v/v), and CH_2Cl_2/hexane (4/1, v/v), to yield residue R2. After each extraction, supernatants were combined in the separatory funnel; after final extraction (CH_2Cl_2/hexane) the funnel contents separated into a bottom organic phase and an upper aqueous phase. The organic phase was removed, and the aqueous phase back-extracted with CH_2Cl_2 (2×). All CH_2Cl_2 fractions were combined to yield extract E2. The aqueous layer was left standing over a small volume of residual CH_2Cl_2 in the separatory funnel; fine suspended materials in the aqueous phase collected at the CH_2Cl_2/aqueous layer interface. These materials were collected and archived as E2 "fluff".

Acid hydrolysis. R2 was heated to 55°C in 85% phosphoric acid for 13 days without stirring. The insoluble residue was then separated by filtration (polycarbonate membrane; pore size, 0.4 μm) and extracted as above. The filtrate and all solvent extraction supernatants were combined and partitioned in a separatory funnel as described above; these procedures resulted in extract E3, residue R3, and E3 "fluff".

Analytical techniques

Light microscopy. Initial materials and R1, R2, and R3 were optically characterized using a Zeiss Axioskop equipped with differential interference contrast (DIC). A Zeiss MC-100 camera system and Kodak Technical Pan film were used for photomicrography.

FTIR microspectroscopy. Infrared transmission spectra were acquired on a Nicolet/Spectra-Tech IRμs/SIRM (scanning infrared microprobe) from 600–4000 cm^{-1} using a triangular apodization function and a resolution of 4 cm^{-1}. Objectives were either 32× (0.65 NA) or 15× (0.58 NA) Reflachromat (reflecting Cassegrainian type) and the condensor was a 10× (0.71 NA) Reflachromat. The detector was a liquid-nitrogen-cooled, narrow-band MCT. Sample spectra were obtained by co-adding a number of scans (128 for high signal-to-noise samples and 256 or 512 for small, low signal-to-noise samples) and ratioing the sample scans to the background scans. Samples were prepared by placing a small amount of material on a BaF_2 or KCl plate. A second salt plate was placed on top of the first and the entire arrangement was housed in a micro-compression cell. The sample could then be flattened until it became transparent (~5–15 μm in thickness). A small crystal of KBr was also placed in the cell and used for background spectra. All samples were doubly apertured (above the sample to define the sampling area and below to eliminate stray light effects) with variable rectangular apertures. Sample sizes varied from 20×20 to 100×100 μm. For each of the dinoflagellate residues, spectra were obtained from the walls of a single, isolated, empty resting cyst to distinguish this material from other cellular debris in the samples.

Elemental analysis. C, H and N contents for all residues were obtained on a Perkin Elmer 2400 CHN Elemental Analyzer. The limited quantity of material derived from dinoflagellate cultures precluded duplicate analyses. However, in a parallel study involving Oak pollen (unpublished results), Oak Initial and Oak R1 were analyzed in triplicate, and showed less than 1% variation between measurements, despite large differences in sample size.

Lipid analysis. Concentrated E1 was prepared for GC and GC/MS by first adding anhydrous sodium sulfate (Na_2SO_4) to remove any residual water. The extract was then filtered (Gelman Acrodisc teflon PTFE filter; pore size, 0.45 μm), combined with 2 ml of MeOH/HCl (95/5, v/v), and purged with N_2 before sealing in a sample vial with a Mininert™ vial cap. Transesterification (methanolysis) was performed at 70°C for 14 h. On cooling, 1 ml of H_2O was added and the aqueous phase was extracted by shaking with hexane (4×, 1 ml) and diethylether (3×, 1 ml). Water was removed from the combined organic (upper) phases by passing over a Na_2SO_4 mini-column, and the resulting anhydrous extract taken to dryness under N_2. After re-dissolving the extract in equal volumes of pyridine and Regisil (BSTFA +1% TCMS), derivatization was performed at 60°C for 15 min. This combination of methanolysis followed by BSTFA derivatization was aimed at converting free and bound fatty acids to corresponding methylesters, and alcohols to trimethylsilyl (TMS) ethers. Analysis by gas chromatography/mass spectrometry was carried out as described below for CuO oxidation products.

Direct ("in-source") temperature-resolved mass spectrometry (DT–MS). Direct temperature-resolved mass spectrometry was performed on a JEOL DX-303 double focusing mass spectrometer equipped with a resistively heated platinum filament Desorption Electron Ionization (DEI) probe. Samples (1 to 5 μg) were applied to the filament as a MeOH suspension. The filament was heated at 2 A min^{-1} from source temperature (180°C) up to 1.5 A (~800°C). Electron Impact (EI) spectra (16 eV) were acquired over a mass range of 20–750 amu, at a scan cycle time of 1 s. Extensive descriptions of DT–MS methods and applications are given by Boon (1992) and Eglinton *et al.* (1996).

Curie-point pyrolysis–gas chromatography–mass spectrometry (Py–GC/MS). Py–GC/MS analysis was performed using a Horizon Curie-point pyrolysis unit, a Hewlett Packard (HP) 5890 Series II gas chromatograph, and a VG AutoSpec-Q mass spectrometer. Samples (15–100 μg) were pyrolyzed for 2 or 5 s on wires with a Curie temperature of either 610°C or 770°C under a helium head pressure of 15 psi. Gas chromatographic separation was achieved on a fused silica column (Restek, 60 m × 0.32 mm I.D.) coated with a methylsilicone (R_{tx-1}) stationary phase (film thickness, 0.5 μm). The GC was programmed from 35°C (5 min. hold) to 320°C (20 min. hold) at 3°C min^{-1}. Electron Impact (EI) mass spectra (55 eV) were acquired over a scan range of 35 to 500 amu at a scan rate of 0.6 s/decade and resolution of 2000.

Cupric oxide oxidation. Alkaline CuO oxidation followed the procedure of Hedges and Ertel (1982), with some modification according to Goñi and Hedges (1992). Approximately 2 mg of R3 was CuO oxidized in the presence of 8% NaOH (~20 ml) for 3 h at 155°C. After oxidation, recovery standards (*trans*-cinnamic acid and ethylvanillin) were added, and the alkaline solution acidified to pH 1 by addition of concentrated HCl. The acidified solution was then extracted with ~50 ml of freshly distilled ether (3×), and the organic phase collected, reduced in a rotoevaporator, and dried under a N_2 stream. Prior to analysis by GC/MS, the extract was dissolved in pyridine (50–100 μl) and derivatized with an equal volume of silylating agent (BSTFA +1% TCMS; Regis Chemical) at 60°C for 15 min.

GC/MS was performed using a HP 5890 Series II gas chromatograph and VG AutoSpec-Q mass spectrometer. On-column injection of the sample (0.5 μl) was accomplished by an HP 7673 autosampler, and chromatographic separation was achieved on a capillary column (J&W, 60 m × 0.32 mm I.D.) coated with a DB-1 stationary phase (film thickness, 0.25 μm). Carrier gas (He) supply was operated in constant mass flow mode with vacuum compensation. The GC was programmed from an initial temperature of 70°C (5 min. hold) to a final temperature of 320°C (20 min. hold) at 4°C min^{-1}. EI mass spectra (50 eV) were acquired over a scan range of 50 to 650 amu at a scan rate of 0.9 s/decade and resolution of 2000. The GC/MS interface temperature was 320°C, and source temperature of the mass spectrometer was 250°C.

RESULTS

Light microscopy

Resting cysts are part of the life cycle of dinoflagellates, and a detailed treatment of this cycle can be found in reviews by Tappan (1980), Walker (1984), Pfiester (1984, 1989), and Pfiester and Anderson (1987). In brief, free-swimming cells are normally haploid, and reproduction consists of simple vegetative division. At this stage, many dinoflagellate species (including *L. polyedrum*) are characterized by an armor (the theca) of interlocking cellulosic plates that encloses the cell. When subjected to environmental stress, motile cells may form non-motile asexual temporary cysts (also known as pellicle cysts), which revert to the motile form when favorable growth conditions return. Occasionally, and for reasons not well understood, vegetatively dividing cells produce gametes which fuse to form a diploid motile zygote (the planozygote). Except for being larger in size, planozygotes often closely resemble vegetative cells. In some species, however, the planozygote ultimately loses motility, sheds its theca, and develops one or more new wall layers to become a hypnozygote, or resting cyst. After a period of obligate dormancy, hypnozygotes germinate and the excysting cell undergoes a meiotic division. The exact timing and nature of this division, however, are not always clear. The resulting daughter cells are motile and resume vegetative growth to complete the life cycle.

Figure 3 shows the appearance of dinoflagellate materials before and after each stage of the treatments used to isolate resting cyst walls. Unprocessed residue from culture tubes of *L. polyedrum* consisted chiefly of empty thecae at various stages of dissociation, but also contained cellular debris from all stages of the life cycle including resting cysts, intact motile cells (both vegetative and planozygotic), gametes, ecdysed cells, temporary cysts, and various dispersed cytoplasmic components (Fig. 3(a)). Initial washing, freeze-drying, and solvent extraction of the dinoflagellate material resulted in an R1 showing no significant changes in visual composition, aside from the physical disruption and dispersion of cellular materials (Fig. 3(b)). Formerly intact resting cysts and other cell types were largely disrupted, thecae tended to dissociate into individual plates, and cytoplasmic materials were widely dispersed. Similarly, saponification did little to change the overall visual composition of the

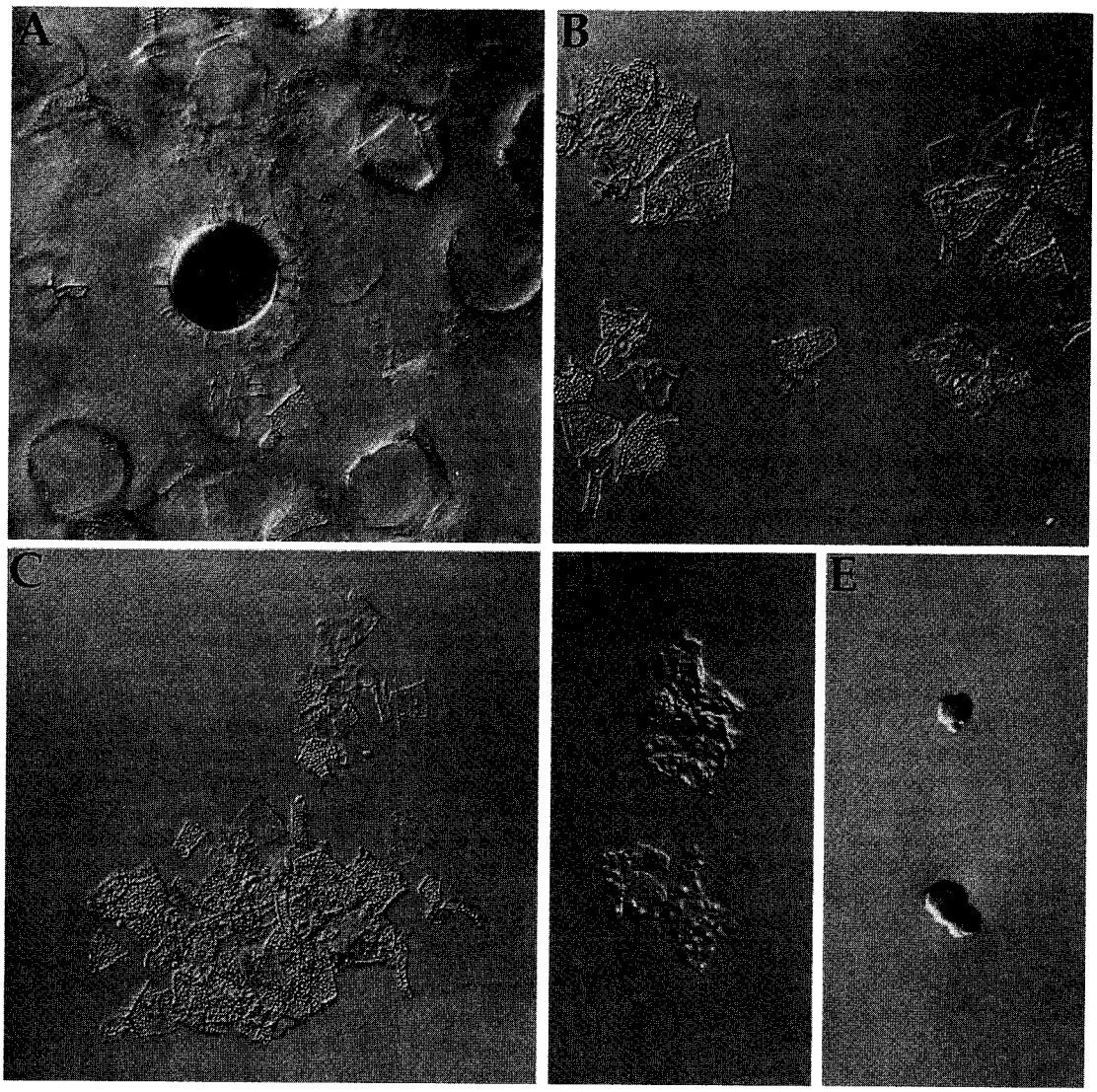

Fig. 3. *Lingulodinium polyedrum* culture materials at each stage of the isolation procedure. (a) Unprocessed culture debris showing a living resting cyst (spiney sphere, ~50 μm in diameter, just left of center) surrounded by empty thecae and culture medium. (b) R1 (residue after sonification and solvent extraction). Culture debris disrupted and dispersed; residue consists mostly of dissociated thecal plates. Note sheet of resting cyst wall (with spines sheared off) visible at lower right. (c) R2 (residue after saponification). Optically identical to R1. Note folded sheet of cyst wall at top of photo. (d) R3 (residue after acid hydrolysis). At this stage, residue consisted almost entirely of isolated sheets of resting cyst wall material. Typically, spines either folded, flattened, or sheared off during processing. (e) Irregular to globular bodies, rare but present in R3.

residue (Fig. 3(c)). After acid hydrolysis, however, the character of the residue changed dramatically (Fig. 3(d)). R3 consisted almost entirely of random-sized sheets of resting cyst walls, clearly identifiable by their characteristic "fibrous" wall texture, archeopyle sutures, and spines. Resting cyst walls at this stage appeared light amber in color, a noticeable change from the greyish translucence shown in R2 (i.e., pre-acid-hydrolysis.) Also present in R3 were small (generally < 10 μm) globular to irregularly shaped masses that are of uncertain origin, but with a morphology that is clearly different to that of the outermost wall material (Fig. 3(e)). These masses constitute only a minor component of the overall residue (<~3%, visual estimation). No walls or membranes from other life cycle stages could be identified in R3.

FTIR microspectroscopy

FTIR spectra of dinoflagellate materials at all stages of the isolation protocol are shown in Fig. 4 and illustrate the evolution of functional group chemistry as a result of solvent extraction, saponification, and acid hydrolysis.

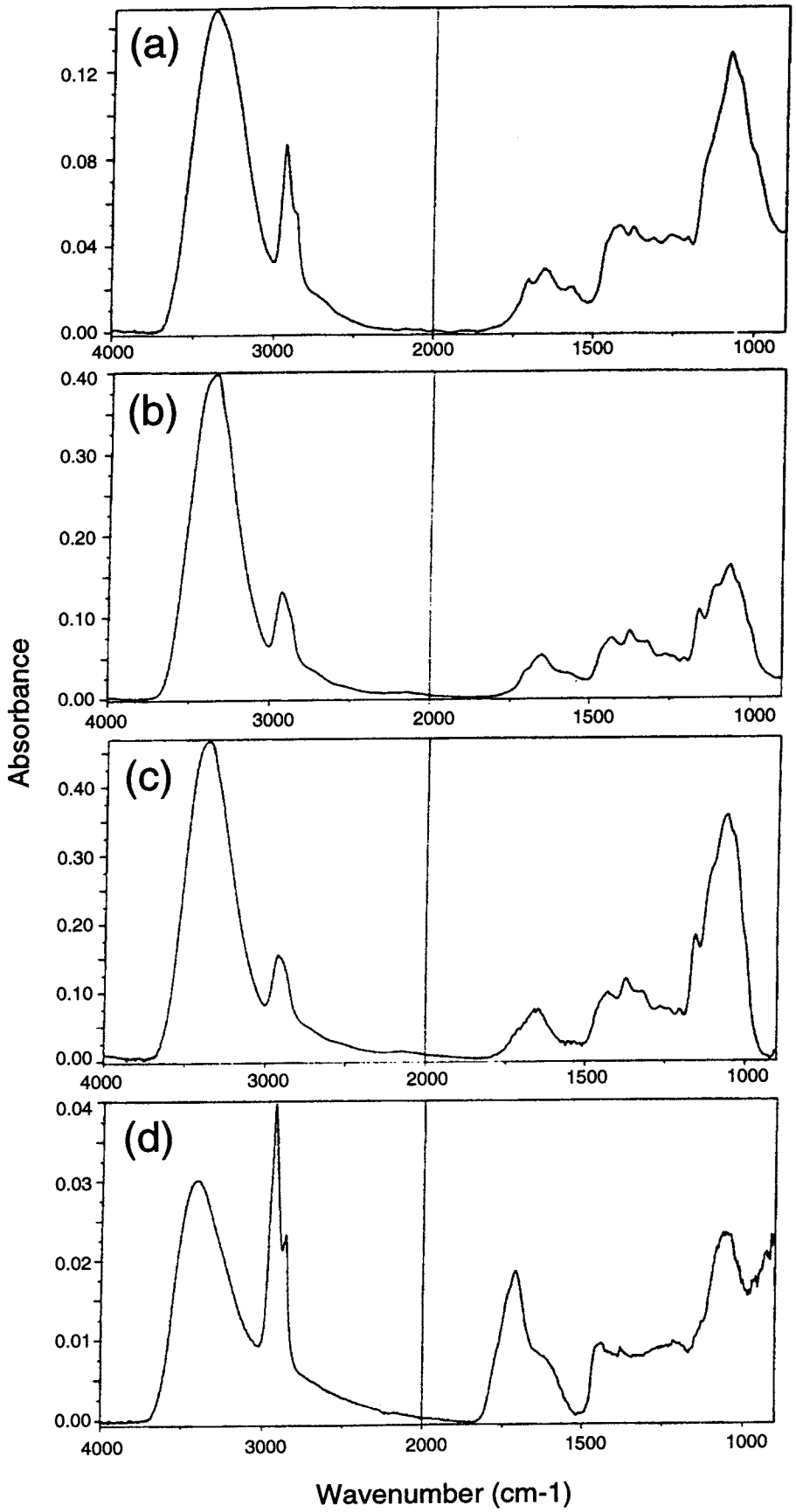

Fig. 4. FT-IR spectra, each obtained from a single resting cyst isolated from (a) initial culture materials, (b) R1, (c) R2, and (d) R3.

A single empty *L. polyedrum* resting cyst isolated from the initial dinoflagellate culture material (after washing and freeze-drying) yielded the spectrum shown in Fig. 4(a). The broad band centered at 3380 cm^{-1} represents hydroxyl groups (primarily phenolic, alcoholic, and/or carboxylic OH, but any remaining free water would also contribute to this absorbance). A sharp absorption at 2929 cm^{-1}, and a weaker one at about 2855 cm^{-1}, relate to CH_2 and/or CH_3 groups. At slightly lower wavenumbers, the very weak and broad absorbance centered at about 2700 cm^{-1} probably results from the presence of carboxylic acid dimers. The carbonyl stretch in carboxylic acid gives rise to the absorbance at 1702 cm^{-1}, while nearby bands at 1654 and 1560 cm^{-1} probably relate to amide C=O and amide N–H bonding, respectively. Absorptions in the interval from about 1450 to 1200 cm^{-1} are difficult to assign with any certainty aside from that at 1374 cm^{-1} which likely relates to CH_2 and/or CH_3 groups. Finally, the strong absorption with a maximum at 1077 cm^{-1} indicates a C–O stretch in carboxylic acid groups.

The spectrum of an empty resting cyst isolated from R1 (Fig. 4(b)) was essentially identical to the initial spectrum aside from small shifts in the wavenumbers of some absorbances, resolution of additional minor bands in the 1100 to 1160 cm^{-1} region, and a decrease in the relative intensity of the CO band at 1063 cm^{-1} and of the OH band. Similarly, the spectrum of post-saponification resting cyst walls (Fig. 4(c)) shows no real change except for some loss of definition of absorbances at 1700 and 1560 cm^{-1}.

A spectrum obtained from sheets of resting cyst walls in R3 is shown in Fig. 4(d). The OH and CO absorptions are still prominent (3415 and 1063 cm^{-1}) but significantly reduced relative to the sharp CH_2 and/or CH_3 absorptions at 2929 and 2860 cm^{-1}. A strong absorption at 1710 cm^{-1} indicates the presence of C=O groups, possibly from carboxylic acid groups. This band shows a broad shoulder in the vicinity of 1630 cm^{-1} which may be due to aromatic and/or olefinic C=C, although other groups (free water, amide C=O) could make some contribution.

Elemental analysis

Values for % carbon, hydrogen, and nitrogen are shown in Table 1. Approximate values for % oxygen are also included, but these were arrived at by difference and therefore probably represent overestimates of the amount of oxygen present (no determination of ash or moisture content was attempted in this investigation). Atomic ratios were calculated using the above elemental data and are also included in Table 1.

Percentage values for all three assayed elements showed no meaningful change throughout solvent extraction and saponification treatments, remaining at ~42% C, 10% N, 4.5% H. After acid hydrolysis, however, the percentages of carbon and hydrogen increased significantly (to ~53% and 9%, respectively), while that of nitrogen showed a marked decrease to ~1%. These changes resulted in an increase in H/C ratio from ~1.3 to nearly 2, and a decrease in N/C from 0.16 to 0.02.

Lipid analysis

The total ion chromatogram (TIC) resulting from GC/MS analysis of E1 is shown in Fig. 5. Peak numbers correspond to the compounds listed in Table 2. The dominant compounds in this chromatogram are a series of fatty acids of even carbon number ranging from C_{14} to C_{24}, with a strong maximum at C_{16} (Peak #3, scan 1125). Other significant components include a full suite of tocopherols (α-tocopherol, Peak #16, scan 2249; γ-tocopherol, Peak #14, scan 2193; δ-tocopherol, Peak #12, scan 2130) listed here in order of decreasing abundance. Sterols are well represented, the most abundant being cholesterol (Peak #9, scan 2042) and dinosterol (Peak #15, scan 2207). Other sterols tentatively identified include 4-nor-dinosterol (Peak #13, scan 2158) and gorgosterol (Peak #17, scan 2334). Also noteworthy are Peaks #6 and #10 which correspond to C_{18} and C_{28} alcohols, respectively.

Direct temperature–resolved mass spectrometry (DT–MS)

Total ion current (TIC) profiles. TIC thermal evolution profiles resulting from direct mass spectrometry of the *L. polyedrum* materials are shown in Fig. 6. Pyrolysis of unprocessed culture residue

Table 1. Elemental analysis of *Lingulodinium polyedrum* cell residues

	Initial	R1	R2	R3
%C	43.12	44.02	41.66	52.73
%N	10.06	12.53	8.14	1.25
%H	4.60	4.77	4.40	8.64
%O[a]	42.22	38.68	45.80	37.38
H/C	1.270	1.293	1.254	1.948
O/C	0.735	0.658	0.826	0.530
N/C	0.200	0.244	0.166	0.020

[a]Calculated by difference; values for H and O not corrected for influence of water or mineral ash.

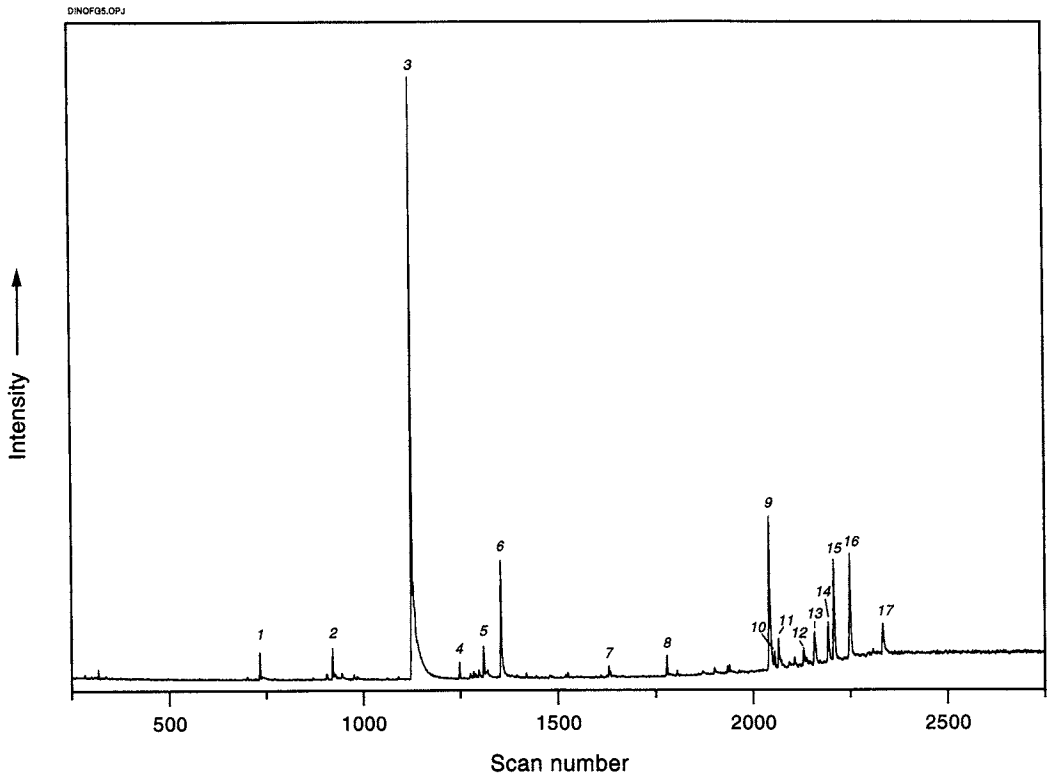

Fig. 5. Total ion current (TIC) chromatogram from GC/MS analysis of E1 (TMS derivatives). Peak numbers correspond to compounds listed in Table 2.

(Fig. 6(a)) yielded three maxima in the TIC trace: the first results from thermal desorption (evaporation) of compounds, and the other two at higher temperatures from thermal dissociation (pyrolysis). After solvent extraction, the desorption maximum was no longer visible (Fig. 6(b)). Saponification further modified the TIC profile by eliminating the secondary pyrolysis maximum (Fig. 6(c)). Pyrolysis of R3 materials (i.e., after acid hydrolysis) yielded the single TIC peak shown in Fig. 6(d). Although similar in basic outline to Fig. 6(c), the R3 TIC peak showed two significant differences: (1) the R3 TIC maximum occurred at a higher temperature (scan 41), relative to that of R2 (scan 38), and (2) the R3 TIC peak is narrower. Thus, acid hydrolysis selectively removed those compounds represented by the lower temperature portion of the TIC curve in Fig. 6(c).

Table 2. GC/MS data for *Lingulodinium polyedrum* extract E1. Compound numbers refer to peak labels in Fig. 5

Compound number	Scan number	Compound name
1	733	hydroxy C10 fatty acid (or hydroxy C12 di-acid)
2	921	C14 fatty acid
3	1125	C16 fatty acid
4	1248	unknown
5	1309	C18 fatty acid
6	1353	C18 alcohol
7	1630	C22 fatty acid
8	1779	C24 fatty acid
9	2042	cholesterol
10	2056	C28 alcohol
11	2066	cholestanol
12	2130	δ-tocopherol
13	2158	4-nor-dinosterol
14	2193	γ-tocopherol
15	2207	dinosterol
16	2249	α-tocopherol
17	2334	gorgosterol?

Summed spectra. The average spectrum of initial dinoflagellate culture material summed over scans 15–50 (Fig. 7(a)) was largely dominated by ions representing polysaccharide fragments (e.g., m/z 57, 60, 73, 98, 126 and 163), a result entirely consistent with our microscopical observation of abundant thecae in the initial sample. Indeed, supplemental analysis of these initial materials using ammonium chemical ionization (NH_3^+–CI) DT–MS (unpublished results) clearly revealed the presence of a relatively pure hexose polymer.

Other prominent ions (m/z 271, 287, 316, 366, and 384) in the initial material spectrum suggest the presence of sterols, while those at m/z 213, 239, and 256 reflect free and bound fatty acids. A series of tocopherols are indicated by ions at m/z 402, 416, and 430. Ions at m/z 522, 550 and 578 most likely represent M^+-18 fragments of bound fatty acids (as diglycerides) incorporating pairs of $C_{16}+C_{14}$, $C_{16}+C_{16}$, and $C_{16}+C_{18}$ units respectively. The presence of these compounds in the initial material

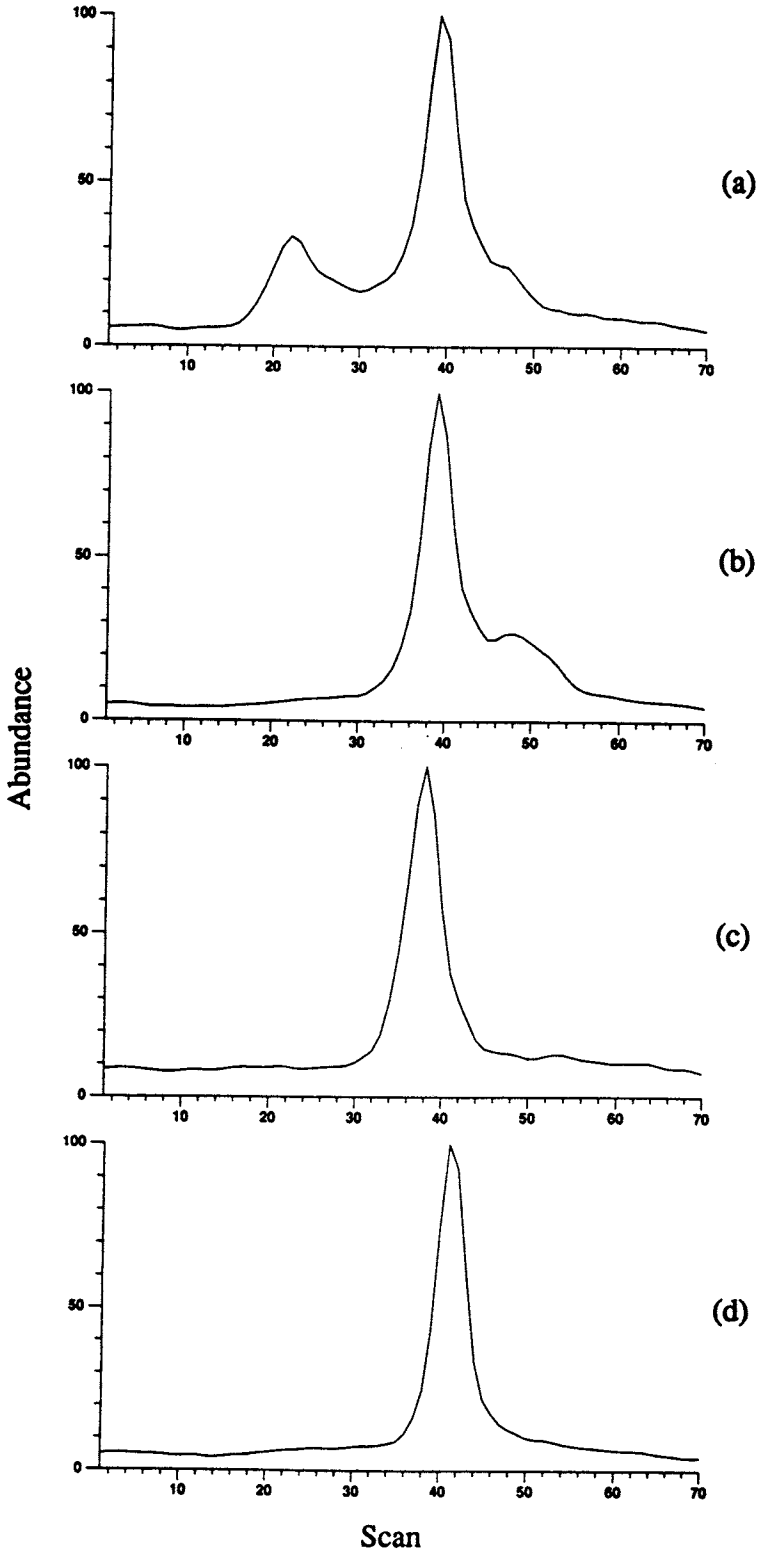

Fig. 6. Thermal evolution profiles of total ion current (TIC) intensity from DT–MS analysis of *L. polyedrum* materials: (a) Initial, (b) R1, (c) R2, and (d) R3.

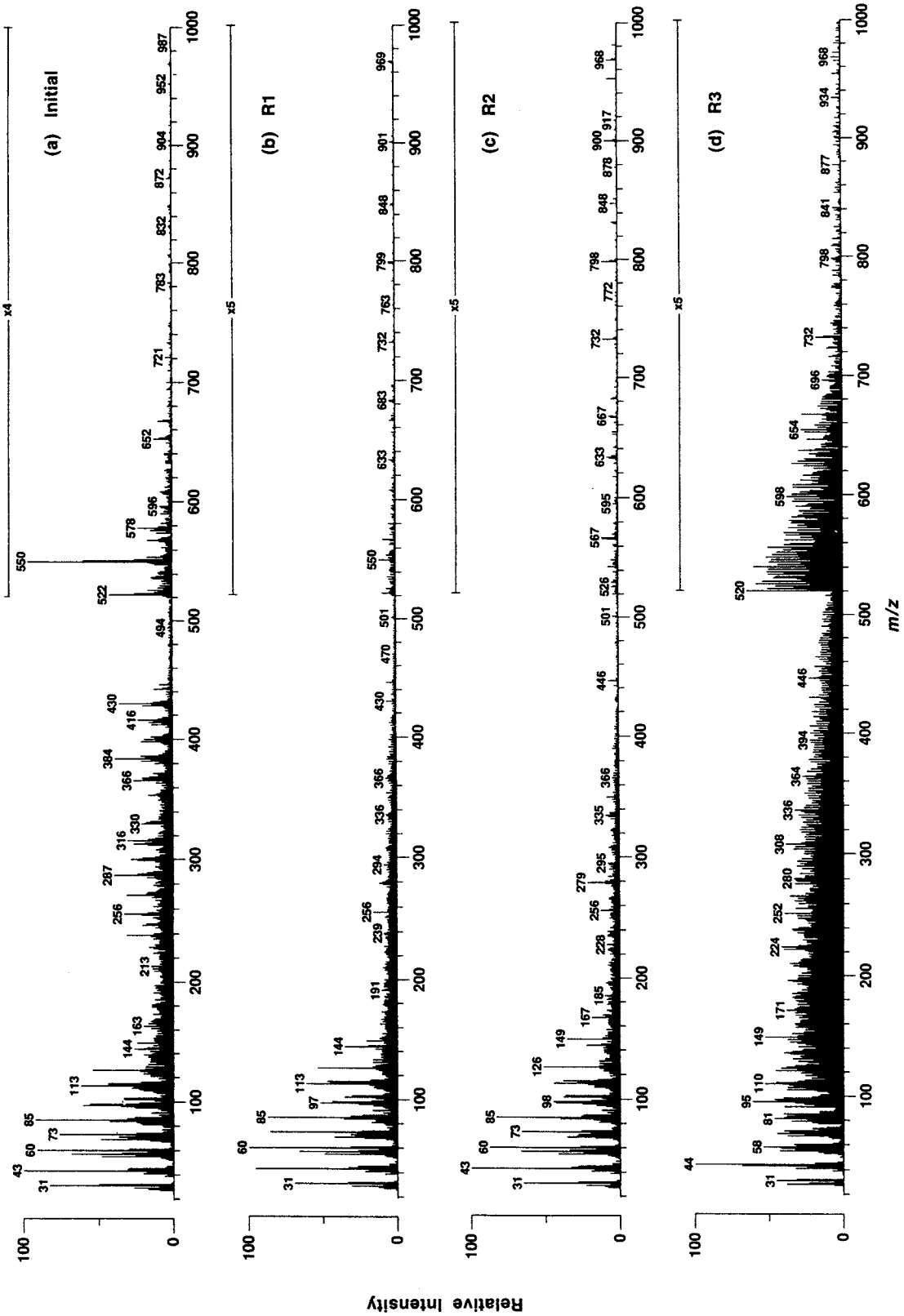

Fig. 7. DT–MS spectra (EI, 16 eV) summed over entire thermal evolution profile for (a) Initial, (b) R1, (c) R2, and (d) R3.

nicely supports the distribution and abundance of fatty acids, sterols, and tocopherols identified by GC/MS in E1.

Ions of polysaccharide fragments again dominated the summed spectrum of R1 (Fig. 7(b)) implying the insolubility of the polysaccharides in the solvents used for lipid extraction. Sterols, however, were largely removed, with the possible exception of some residual dehydrated sterol suggested by the ion at *m/z* 366. Fatty acids also continue to contribute to the spectrum as shown by the presence of ions at *m/z* 228 ($C_{14:0}$), 239 (ester bound $C_{16:0}$), and 256 ($C_{16:0}$). The spectrum of R2 (Fig. 7(c)) is very similar to that of R1 indicating that the post-saponification residue still consists mainly of polysaccharides. Ions at *m/z* 149, 167, and 279 probably represent phthalate (plasticizer) contamination, while that at *m/z* 446 most likely relates to instrument background contributions (Santovac® vacuum pump oil).

DT–MS of the dinoflagellate material after acid hydrolysis yielded a complex spectrum (Fig. 7(d)) showing a bias towards ions of low mass number. The polysaccharide signature present in Initial, R1, and R2 spectra could no longer be detected at this stage. Of those assignable, the most abundant ion (*m/z* 44) represents CO_2, presumably derived from carboxylic acid groups by thermally induced decarboxylation. Ions at *m/z* 224, 252, and 280 may relate to aliphatic fragments in the C_{16} to C_{24} range, while others — *m/z* 110, 120, and 122 — are suggestive of phenolic compounds (dihydroxybenzene, vinylphenol, and ethylphenol, respectively).

Pyrolysis — Gas chromatography/mass spectrometry

Total ion current chromatograms from Curie-point Py–GC/MS analysis of Initial and R3 materials are shown in Fig. 8. Selected peaks are identified in Table 3; these identifications are based largely on comparison of individual peak mass spectra to those in both the literature and standard MS libraries. Recognition of homologous series was aided by mass chromatography of characteristic ions.

Prominent in the TIC trace of the initial material (Fig. 8(a)) are peaks representing polysaccharide pyrolysis fragments, including both early-eluting compounds (lower molecular weight furans, furanones, and pyrans), and later-eluting compounds including 1,4-dideoxy-D-glycero-hex-1-enopyranos-3-ulose and, most abundantly, levoglucosan. Aromatic

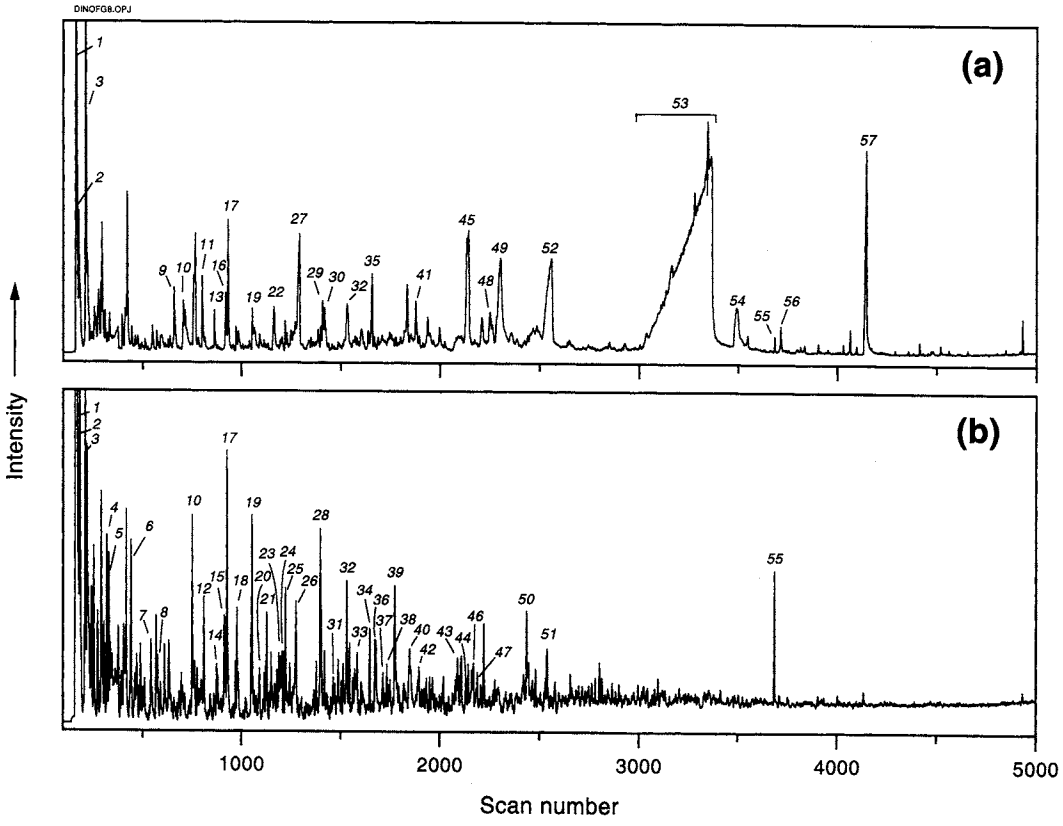

Fig. 8. Partial total ion current (TIC) chromatograms from Curie-point Py–GC/MS analysis of (a) Initial materials, and (b) R3. Peak numbers correspond to compounds listed in Table 3.

Table 3. Py–GC/MS data on *Lingulodinium polyedrum* Initial and R3 materials. Compound numbers refer to peak labels in Fig. 8

Compound number	Compound name
1	carbon dioxide
2	nC4 alkene + alkane
3	nC5 alkene + alkane
4	nC6 alkene
5	nC6 alkane
6	benzene
7	nC7 alkene
8	nC7 alkane
9	alkylfuran?
10	toluene
11	cyclopentanone
12	methylpyran
13	furaldehyde
14	nC8 alkene
15	nC8 alkane
16	cyclopentanone
17	furaldehyde
18	methylvinylfuran
19	C_3-furan
20	ethylbenzene
21	1,3 + 1,4-dimethylbenzene
22	furan-2-one
23	styrene
24	1,2-dimethylbenzene
25	C4-furan?
26	unknown
27	hydroxycyclopent-2-ene-1-one
28	benzaldehyde
29	methyl furaldehyde
30	methyl pyranone
31	C3-benzene
32	phenol
33	C3-benzene
34	hydroxymethylcyclopentanone
35	hydroxymethylcyclopentanone
36	methylfuran + cyclopentanone
37	C4 benzene
38	indene
39	acetophenone
40	methylphenol
41	levoglucosenone + hydroxymethylpyranone
42	C4 alkylbenzene
43	C5 benzene + methylindene
44	C5 alkylbenzene
45	unknown
46	C6 alkylbenzene + C2 phenol
47	naphthalene
48	dianhydrolucopyranose
49	5-hydroxymethyl-2-furaldehyde
50	dihyroinden-1-one
51	C2-dihydroindene
52	1,4-dideoxy-D-glycero-hex-1-enpyranos-3-ulose
53	levoglucosan
54	anhydro-β-D-glucofuranose
55	prist-1-ene
56	C14:0 fatty acid
57	C16:0 fatty acid

compounds such as toluene (Peak #10) and phenol (Peak #32) are minor products. A major component (Peak #57) is identified as a $C_{16:0}$ fatty acid, while spectra obtained for several high molecular weight peaks (not shown in Fig. 8) suggest the presence of sterols.

Peaks representing sterols and fatty acids are not detectable in the R3 Py–GC/MS TIC chromatogram shown in Fig. 8(b). The strong polysaccharide signature of the initial material has also been significantly reduced, but not eliminated entirely as indicated by the continued presence of furan and furanone peaks. Pyrolysis of R3 produced a more prominent and extensive series of aromatic compounds including naphthalenes, indanes, indenes, and benzaldehydes as well as alkylbenzenes and phenols. The strong signal at Peak #55 was identified as 2,6,10,14-tetramethyl pentadec-1-ene (prist-1-ene).

Cupric oxide (CuO) oxidation

A total ion current (TIC) chromatogram showing reaction products from alkaline cupric oxide oxidation analysis of R3 is shown in Fig. 9; peak numbers correspond to tentative identification of compounds as listed in Table 4. Major aromatic products revealed by GC/MS include benzoic acid (Peak #1), carboxylated phenols (Peaks #16 and #18), and *ortho*, *meta*, and *para* isomers of hydroxybenzoic acid (Peaks #8, #11, and #14, respectively). A series of short chain (C_4–C_6) diacid products are represented by peaks #3, #6, and #7. Other aliphatic products include dihydroxy C_{10} and C_{11} fatty acids (Peaks #20 and #22).

DISCUSSION

In this paper, we report the results of the first extensive chemical characterization of the highly resistant cell wall material enclosing a dinoflagellate resting cyst. Studies of these walls are complicated by the fact that they are produced only by a small number of extant species, and then only during certain stages of the life cycle. As a result, the task of generating sufficient quantities of sample for rigorous chemical analysis requires a considerable investment in culturing the species of interest, and understanding the nature and timing of various life cycle events. Alternative strategies which involve the study of preserved cyst walls of species from the fossil record (de Leeuw *et al.*, 1993) are complicated by the challenge of cleanly isolating and concentrating the material from its host matrix, and also involves the question of chemical (diagenetic) changes incurred by the cysts during fossilization. The study reported here follows a 5-year investigation of the experimental organism (*L. polyedrum*) in laboratory culture, with emphasis on the morphological development and ultrastructure of resting cysts (Kokinos, 1994; Kokinos and Anderson, 1995). Thus, the biological origin and significance of the cellular materials under investigation are well characterized, and provide a solid foundation from which to explore chemical composition.

Evaluation of cyst wall isolation efficiency and processing artifacts

A critical component of studies seeking to characterize the resistant walls of extant plant cells is the nature of the isolation procedure. An ideal

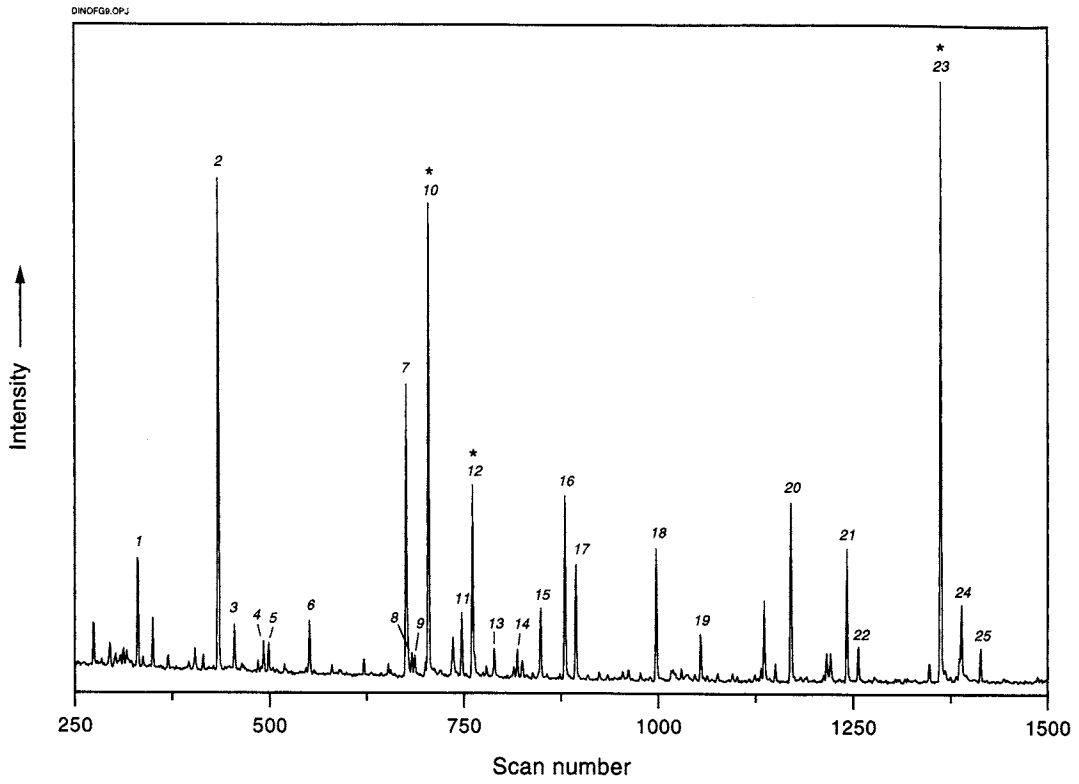

Fig. 9. Total ion current (TIC) chromatogram showing CuO oxidation reaction products (TMS derivatives) of R3 as revealed by GC/MS. Peak numbers correspond to compounds listed in Table 4 (*Internal standard).

protocol would meet two objectives, (1) isolate a pure residue of the cell wall material by elimination of all other cellular (and extracellular) substances, and (2) accomplish this isolation without modification of wall chemistry. The extent to which these objectives can both be met is currently difficult to assess. Early investigations of dinoflagellate cysts, pollen, and spores often accomplished wall isolation using relatively drastic chemical techniques such as acetolysis (i.e., boiling in acetic anhydride/concentrated sulfuric acid, ~9/1, v/v, for ~10–20 min.; see Erdtman, 1961). Although generally yielding "clean" wall preparations, this technique has more recently been suspected to alter the composition of the walls to such an extent as to make original components difficult or impossible to chemically identify. Berkaloff *et al.* (1983) concluded that acetolysis resulted in partial acetylation of hydroxyl groups which greatly complicated IR analysis and subsequent use of spectra for comparative purposes. Furthermore, acetolysis of unextracted materials can produce artifacts due to the condensation of carotenoids and other lipids into resistant clumps which, again, may hamper analysis by IR and other methods (Brunner and Honegger, 1985). Direct acetolysis of our dinoflagellate materials (Kokinos, 1994) yielded a substance having FTIR and DT–MS characteristics very different from those of the R3 residue described herein.

Table 4. Alkaline CuO oxidation products of residue R3 as revealed by GC/MS. Compound numbers refer to peak labels in Fig. 9. (I.S. = internal standard)

Compound number	Compound name
1	benzoic acid
2	butane-1,4-dioic acid + unknown aromatic
3	C4 diacid (branched)
4	*p*-hydroxybenzaldehyde
5	C9 fatty acid
6	pentane-1,5-dioic acid
7	hexane-1,6-dioic acid
8	*o*-hydroxybenzoic acid
9	vanillin
10	*trans*-cinnamic acid (I.S.)
11	*m*-hydroxybenzoic acid
12	ethylvanillin (I.S.)
13	heptane-1,7-dioic acid?
14	*p*-hydroxybenzoic acid
15	C12 fatty acid
16	carboxy–hydroxy benzaldehyde
17	octane-1,8-dioic acid
18	nonane-1,9-dioic acid + 2-carboxy-4-hydroxybenzaldehyde
19	tetradecanoic acid
20	Di–OH C10 fatty acid?
21	hexadecanoic acid
22	Di–OH C11 fatty acid?
23	internal standard
24	octadecenoic acid
25	octadecanoic acid

To avoid the drawbacks of direct acetolysis, many recent studies (e.g., Berkaloff *et al.*, 1983; Largeau *et al.*, 1984, 1986; Burczyk, 1987a,b; Puel *et al.*, 1987; Burczyk and Dworzanski, 1988; Goth *et al.*, 1988; Guilford *et al.*, 1988; Kadouri *et al.*, 1988; Derenne *et al.*, 1989, 1990, 1991; Gelin *et al.*, 1996) have employed successive chemical treatments patterned to various degrees after those of Zetsche *et al.* (1937) and Shaw and Yeadon (1966). Typically, these treatments consist of (1) solvent extraction, (2) saponification via KOH reflux, and (3) acid hydrolysis (phosphoric or sulfuric acid), designed to liberate free (lipid), esterified, and more tightly-bound components respectively. Many of the investigations employing such an approach have sought to elucidate the nature of resistant biopolymers produced by various microalgae. To allow comparison of our results to these studies, we adopted the above treatments, basing details on the scheme provided by Tegelaar (1990). It should be noted, however, that alternative isolation strategies, involving various mild chemical pre-treatments (Allard *et al.*, 1997), or the use of enzymes to remove specific cellular materials (Schultze Osthoff and Weirmann, 1987; Wehling *et al.*, 1989; Mulder *et al.*, 1992), have been applied by some investigators in microorganism and pollen studies respectively, and show great potential for obtaining pure cell wall fractions while avoiding artifacts from aggressive acid/base treatments.

Our solvent extraction procedure was aimed at the release of free (i.e., unbound) lipids. Since lipids typically comprise only a few percent of the cellular biomass, we did not see significant changes in bulk parameters such as optical character and elemental composition. In contrast, one might predict that removal of long chain fatty acids via solvent extraction could impact FTIR spectra to some extent by reducing any aliphatic signature. This may explain why the FTIR spectrum of R1 shows a weaker CH_2+CH_3 absorbance (relative to the wide OH band at $\sim 3360\,cm^{-1}$) compared to the corresponding spectrum of unprocessed materials (Fig. 4(a), (b)). The mass spectrum produced by DT–MS analysis of R1 indicates a significant reduction of fatty acids, sterols, free tocopherols, and diglycerides as a result of solvent extraction. These changes are consistent with the reduction of ion intensity at lower temperatures in the desorption TIC profile of R1 (Fig. 6(b); Eglinton *et al.*, 1996).

Reflux in KOH, followed by acidification and extraction, was employed to cleave ester bonds and remove the released hydrolysis products. Saponification of R1 had no significant impact on the optical character of this material. Similarly, virtually no change could be detected with the FTIR analysis of R2. Although the TIC trace resulting from DT–MS of R2 shows some modification in the shape of the high temperature pyrolysis peak, little change could be detected in the mass spectrum relative to that of R1.

Acid hydrolysis was utilized to remove polysaccharides (by cleavage of glycosidic linkages) and proteinaceous materials (by cleavage of peptide bonds). Since the bulk of the dinoflagellate material up to this point consisted of cellulosic thecal plates, we anticipated marked changes in bulk properties from treatment with phosphoric acid. Indeed, optical analysis of R3 indicated complete removal of thecal plates and all other cellular components with the exception of the trace quantities of globular/irregular bodies noted above. This major change in optical character was reflected in results from other analyses of the final residue, all of which documented the substantial removal of polysaccharides during acid hydrolysis. Elemental analysis of R3 showed major changes in bulk composition. For example, the marked decrease in N/C is consistent with the anticipated hydrolysis of amide bonds (e.g. in peptides). FTIR analysis of isolated sheets of resting cyst wall material indicated a significant decrease in OH peak intensity, consistent with the loss of polysaccharides from the cell wall. Similarly, both the high temperature shift of the DT–MS TIC profile maximum and the elimination or partial reduction of specific mass peaks from the DT–MS spectrum suggest major changes in the composition of the dinoflagellate material, again consistent with removal of polysaccharides.

Overall, our results show that solvent extraction, saponification, and acid hydrolysis treatments had the intended effect of sequentially removing characterizable biochemicals from initial culture-derived materials. Furthermore, knowing the types of chemical linkages susceptible to these treatments, we can postulate that any remaining materials (i.e., R3) are cross-linked by fairly recalcitrant bonds — such as carbon–carbon or ether bonds. Direct gravimetric assessment of products associated with the isolation procedure, and particularly the R3 yield, was difficult in the present study due to the limited quantity of material. In general, no major reduction in sample size was observed from the initial quantity prior to acid hydrolysis. The final yield of R3 is roughly estimated to be ~1–2% (on a dry weight basis) of the initial *L. polyedrum* culture sample.

A second major consideration of the isolation protocol concerns the possibility that resistant cell wall materials themselves become chemically modified during one or more of the isolation treatments, or that partial hydrolysis products of proteins and polysaccharides may react with one another, leading to the formation of resistant artifacts (Allard *et al.*, 1997). We draw upon the following evidence to argue that the R3 material resulting from the isolation procedure employed is authentic.

First and foremost, light microscopy studies revealed that R3 almost entirely consisted of material that was morphologically and texturally identical to the outer cyst walls observed in the initial material as well as those isolated by traditional palynological methods (acetolysis; Kokinos, 1994). Moreover, from a quantitative standpoint, the low overall yield of R3 residue (~1%) is consistent with visual estimates of cyst wall material in the initial sample. The small globular bodies that were also observed in R3 constituted only a trace constituent (<3%) of the residue, and may indeed also be authentic (as opposed to artifactual) in origin. These results contrast sharply with reports of amorphous residues observed in bacterial cell wall isolates (Flaviano *et al.*, 1994) which have recently been attributed as artifacts from "Malliard-type" condensation reactions (Allard *et al.*, 1997). Second, the sharp reduction in the atomic N/C ratio coupled with a lack of recognizable amino acid products from CuO oxidation (Goñi and Hedges, 1993), suggests that protein-derived residues are unlikely to constitute a major fraction of R3. Third, the thermal evolution TIC profiles of the R3 are characterized by a narrow, high temperature (*ca.* 800°C) peak. The elevated temperature for maximum product evolution and the shape of the TIC profile indicate the decomposition of a thermally recalcitrant, and chemically rather homogeneous macromolecule. This would contrast with a broader profile with lower temperature maxima stemming from contamination by protein and polysaccharide condensation residues (Allard *et al.*, 1997). Fourth, in a parallel study, we investigated the chemical composition of resistant organic matter in two pollen samples (Goñi *et al.*, 1998). Because sample availability was not an issue we employed two different chemical isolation schemes; one was identical to that used in the present study and in the second the acid hydrolysis was achieved using a 2 h treatment with concentrated (95%) H_2SO_4. Py–GC–MS of residues from both treatments (not shown) yielded very similar results. While these observations do not provide a direct assessment of the influence of different acid hydrolysis treatments on the dinoflagellate cyst material, they do provide further circumstantial evidence in support of our argument.

Finally, if the structure and composition of R3 materials are an accurate reflection of the parent

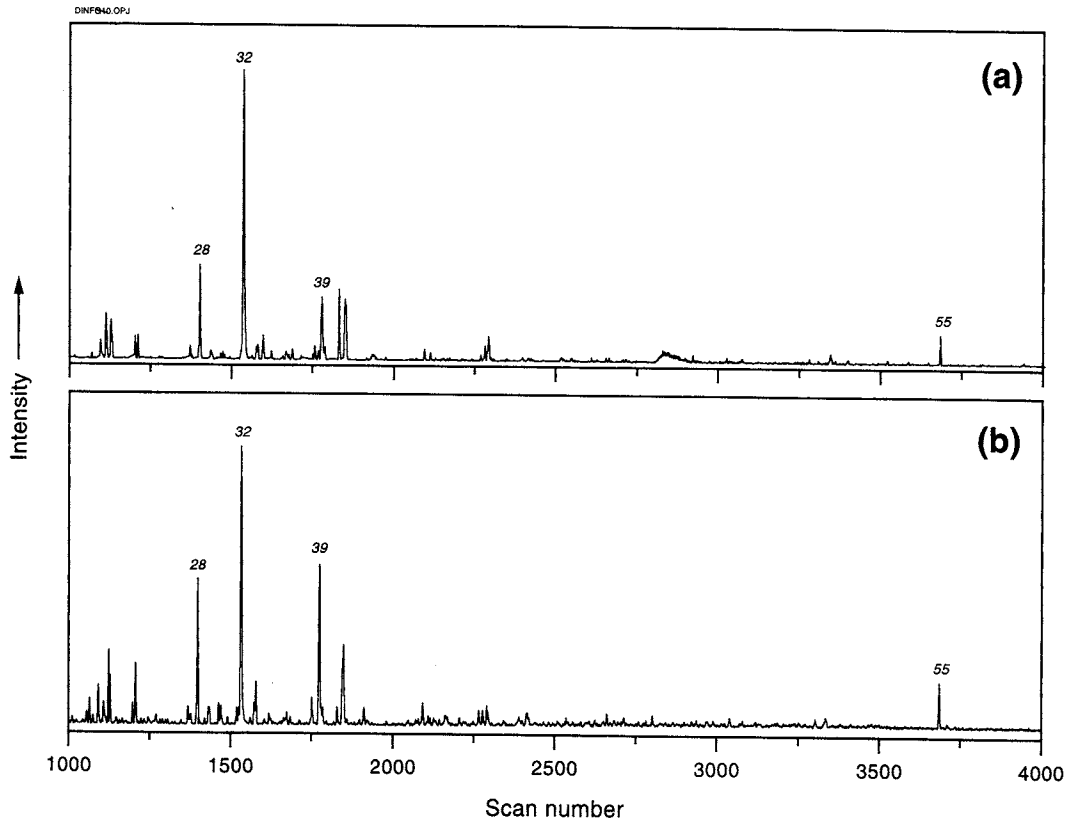

Fig. 10. Partial summed (composite) mass chromatograms showing the presence of selected pyrolysis products generated during Py–GC/MS of (a) initial materials, and (b) R3. Peak numbers correspond to compounds listed in Table 3. Chromatograms were generated by mass chromatography of ions at m/z 94.07 + 106.08 + 108.09 + 120.1 + 126.19 + 266.36.

biomacromolecule(s) the chemical characteristics of R3 should be detectable in the initial material, albeit in trace amounts. To test this assumption, we employed mass chromatography of selected ions characteristic of R3 to selectively enhance the signal of specific pyrolysis products in the Py–GC/MS chromatogram of the initial material. The partial summed (composite) chromatograms shown in Fig. 10 were generated via mass chromatography of ions of m/z 94.07 + 106.08 + 108.09 + 120.1 + 126.19 + 266.36. In these chromatograms, peaks characteristic of the products liberated during R3 pyrolysis (Fig. 8(b): 28 = benzaldehyde; 32 = phenol; 39 = acetophenone, 55 = prist-1-ene) are clearly revealed in the initial dinoflagellate material (Fig. 10(a)). The occurrence of these characteristic pyrolysis products in similar relative abundance before and after application of the isolation treatments provides qualitative evidence that resistant macromolecular substances were originally present in the *L. polyedrum* resting cyst wall and unaltered by the isolation protocol.

In summary, while it is impossible to rule out the possibility of artifacts, we believe there is strong evidence to suggest that a substantial proportion of the R3 residue directly stems from the resting cyst wall material that is the target of this study.

Characterization of R3

With the premise that the R3 is an accurate manifestation of the resting cyst wall (and accepting the caviat that the some proportion of the residue is artifactual in origin), we turn our attention to the question of the chemical nature of the R3 material. For this purpose we first return to the visual description of the isolated residue.

Although, under the light microscope, R3 consisted almost entirely of isolated resting cyst walls the final residue did contain the unusual globular to irregularly shaped masses described earlier. The size and morphology of these bodies suggest a relationship to small globular masses, termed accumulation bodies, occurring in the cytoplasm of some living dinoflagellate species (Taylor, 1968; Schmitter, 1971, 1989; Bibby and Dodge, 1972). These structures can be detected within motile cells, but are most obvious in resting cysts. Although the function of accumulation bodies is unknown, some authors have hypothesized a role in subcellular digestion (e.g., Fritz *et al.*, 1989). The brownish to reddish orange color typical of these bodies has been considered to suggest the presence of concentrated carotenoids (Evitt, 1985), an interesting hypothesis in light of earlier speculation linking the "fossilization potential" of dinoflagellate resting cyst walls to the presence of a "carotenoid-derived" sporopollenin substance.

Structures virtually identical to accumulation bodies are commonly associated with fossilized dinoflagellate cyst walls (including those of fossil *L. polyedrum*) and often have a characteristic species-dependent appearance (Evitt, 1985). Since *L. polyedrum* resting cysts forming in our laboratory cultures showed one or more prominent orange-pigmented accumulation bodies (Kokinos and Anderson, 1995), it is tempting to link these structures to those found in our R3. An unambiguous correlation, however, will likely involve further examination, perhaps analyzing cellular structures with transmission electron microscopy before and after all isolation steps.

The lack of recognizable pellicle structures in both R3 and in acetolyzed dinoflagellate material (Kokinos, 1994) was surprising, given the statement by Morrill and Loeblich (1981) that the pellicular layer of *Gonyaulax polyedra* (now *L. polyedrum*) is resistant to acetolysis. These authors, however, tested two strains of *L. polyedrum*, but only one is indicated to have yielded resistant pellicles. It is possible, therefore, that pellicle resistance is strain-specific. In the present investigation, we expected any pellicular layers surviving acid hydrolysis to be visible during detailed observations of R3 with contrast enhancement microscopy, since (1) initial dinoflagellate culture material contained large numbers of vegetative cells (all of which presumably contained a pellicle layer), and (2) both acetolysis and our 3-step isolation protocol darkened resistant wall layers enhancing their visibility under the microscope. Overall, based on our optical characterization of R3 materials, we conclude that this residue consists almost entirely (~97%) of isolated walls of *L. polyedrum* resting cysts.

FTIR microspectroscopy yielded a unique perspective on R3 since it could be performed on optically identified, isolated particles rather than on total residue. As indicated above, key features of the R3 FTIR profile included absorbances indicative of abundant aliphatic CH_2 and/or CH_3, carboxylic acid C=O, and hydroxyl groups, features which may suggest the presence of long chain fatty acids. Interestingly, our R3 FTIR profile very closely resembles published IR spectra of *Lycopodium* spore cell walls (Rouxhet *et al.*, 1980; Berkaloff *et al.*, 1983; Puel *et al.*, 1987; Geisert *et al.*, 1987). Atkinson *et al.* (1972) also illustrate an IR spectrum of *Lycopodium* spores, but unfortunately resistant materials were obtained by acetolysis, and hence the spectrum is difficult to interpret. An IR spectrum of pollen wing (*Pinus mugo*) sporopollenin isolated with enzymatic treatments has been reported by Schultze Osthoff and Weirmann (1987). This spectrum extends to lower wavenumbers than we were able to obtain under micro-FTIR conditions (625 vs ~950 cm^{-1}), but very closely matches that of our R3. These authors note peaks at 1625, ~1600, ~1500, 1430, and 830 cm^{-1} as being indicative of the presence of aromatic structures. Our R3

spectrum shows similar features in these regions (shoulder in the 1600–1625 cm^{-1} region, peak around 1430–1440 cm^{-1}, weak but detectable response at ~1515 cm^{-1}), and thus may indicate the presence of aromatic components. Puel *et al.* (1987) isolated sporopollenin from another species of *Pinus* (*P. silvestris*) by successive solvent extraction, saponification, and acid hydrolysis; IR analysis of this material yielded a spectrum identical to that of *P. mugo*.

Several published studies describe IR spectra of resistant outer walls isolated from non-dinoflagellate algal species. Many of these (Atkinson *et al.*, 1972; Good and Chapman, 1978; König and Peveling, 1980; de Vries *et al.*, 1983; Delwiche *et al.*, 1989) employed acetolysis as the isolation mechanism and therefore results are not directly comparable to those reported here. Investigations by Berkaloff *et al.* (1983), Puel *et al.* (1987), and Burczyk (1987a), however, isolated resistant cell wall biopolymers from various green algae using techniques similar to those of the present study. In the first two of these investigations, IR spectra were compared to those obtained from traditional sporopollenins (*Pinus* pollen and *Lycopodium* spores). Differences between algal and spore/pollen materials were notable, especially concerning oxygen distribution and degree of unsaturation. On the strength of these IR comparisons, both Berkaloff *et al.* (1983) and Puel *et al.* (1987) conclude that resistant cell wall materials derived from *Botryococcus* and *Prototheca* are distinct in structure and composition from "traditional" sporopollenins.

As shown in Table 1, the H/C ratio for R3 is nearly 2, pointing toward a highly aliphatic structure — an observation somewhat consistent with the FTIR results, but contradictory to pyrolysis and CuO oxidation data (see below). This lack of agreement is difficult to interpret, but may derive from a biasing of elemental data due to water absorption and/or the presence of mineral ash. Given the very limited quantity of R3 available for elemental analysis, even a small amount of absorbed water could have interfered with final results by elevating H/C values. Alternatively, residual polysaccharides in R3 might also serve to artificially elevate the H/C ratio. We attempted analysis by solid state ^{13}C nuclear magnetic resonance (NMR) spectroscopy to further resolve the aliphatic vs aromatic character of R3, however our sample size proved insufficient. Given the potential factors that may have influenced the hydrogen (and oxygen) determinations we consider it imprudent to interpret the data for H and O in a quantitative context.

In our study, DT–MS and Py–GC/MS analyses provided additional criteria for evaluation of chemical structure and composition. Although pyrolysis liberates only a subset of the macromolecular building blocks, recent studies have illustrated that the fragments generated are structurally representative of the parent macromolecule(s) (Larter and Horsfield, 1993).

An unexpected feature of the R3 Py–GC/MS TIC chromatogram was the abundance of peaks representing lower molecular weight furans. Since light microscopy indicated the complete removal of cellulosic thecal materials during acid hydrolysis, we anticipated any polysaccharide signature generated during pyrolysis of R3 to be greatly reduced or eliminated entirely. Interpretations of this phenomenon might draw on one or more of a number of hypotheses. First, the presence of furan peaks may indicate a residual polysaccharide component in R3 which is independent of the original thecal plate materials and physically protected from hydrolysis. Many investigations have described a relatively thick cellulosic layer (the endospore) which is incorporated in the cell covering of some dinoflagellate resting cysts (Evitt, 1985). Such wall layers are a prominent feature of *L. polyedrum* resting cysts, and can be easily detected with both light and electron microscopy (Kokinos, 1994; Kokinos and Anderson, 1995). If polysaccharides in this layer are tightly bound to the overlying resistant cell wall and manage to survive acid hydrolysis, furan products may be among those products generated by pyrolysis. Other hypotheses to explain furan production during R3 pyrolysis invoke artifacts of acid hydrolysis. For example, strong dehydration during acid hydrolysis, or the presence of phosphate residues after this treatment, may have led to "charring" reactions that could result in furan generation during subsequent pyrolysis. Melanoidins, another potential artifact of acid hydrolysis, might also yield furans upon pyrolysis (Larter *et al.*, 1981). To evaluate these latter hypotheses, it would be interesting to compare (via Py–GC) the R3 materials obtained in this study to those isolated with alternative methods (e.g., enzymatic treatments) which do not employ aggressive acid hydrolysis.

Another noteworthy feature of the R3 chromatogram is the prominent peak representing prist-1-ene. This compound has been encountered in investigations of resistant wall biopolymers of the green alga *Tetraedron minimum* (Goth *et al.*, 1988), inner seed coats of fossil water plants (van Bergen *et al.*, 1994a), and also appears ubiquitous in pyrolysates of marine sedimentary kerogens (Larter *et al.*, 1979). There has been considerable interest in the origin of prist-1-ene as a pyrolysis product in geochemical samples (Goossens *et al.*, 1984; Li *et al.*, 1995), and tocopherols and chlorophylls have both been suggested as possible sources. Based on the abundance of tocopherols in the lipid extract of our culture samples, and the lack of chlorophyll pigmentation associated with *L. polyedrum* resting cyst cell walls, a tocopherol origin seems more likely for the prist-1-ene encountered in the present study.

The prominence of prist-1-ene in the TIC chromatogram suggests that tocopherols form an integral part of the *L. polyedrum* resting cyst wall, a conclusion similar to that drawn for the tocopherols associated with fossil seed coats. These findings raise the possibility that bound tocopherols may contribute in some way to the high preservation potential of certain organic cell walls, an intriguing hypothesis in light of the role of tocopherols as anti-oxidants in membrane-protection within living cells (Burton and Ingold, 1986).

Direct comparison of our Py–GC and Py–GC/MS results to those obtained in other studies is somewhat limited by the relatively few reports in which these techniques have been applied to microalgae and the pollen and spores of higher plants. Regarding the resistant cell wall materials of algae, Py–GC data are available for the freshwater chlorophytes *Botryococcus braunii* (Largeau *et al.*, 1984, 1986; Kadouri *et al.*, 1988; Derenne *et al.*, 1989, 1990), *Chlorella fusca* (Derenne *et al.*, 1992), *Scenedesmus obliquus* (Burczyk and Dworzanski, 1988), *S. quadricauda* (Derenne *et al.*, 1991), and *T. minimum* (Goth *et al.*, 1988), the marine chlorophytes *Nannochlorum eucaryotum* (Derenne *et al.*, 1992) and *Chlorella marina* (Derenne *et al.*, 1996), and the marine eustigmatophytes *Nannochloropsis salina* and *Nannochloropsis sp.* (Gelin *et al.*, 1996). The results of all but one of these investigations strongly indicate macromolecular structures comprised chiefly of polymethylenic chains. This highly aliphatic character is typified by pyrolysates of *S. obliquus*, *B. braunii* and *N. salina* all of which are dominated by a homologous series of *n*-alkanes/alkenes with chain lengths extending to C_{32} and beyond, and show striking similarities to pyrolysis products of polyethylene (Burczyk and Dworzanski, 1988). The apparent ubiquity of highly aliphatic, non-hydrolyzable macromolecules in the resistant cell walls of the green algae led Tegelaar *et al.* (1989) to introduce the term "algaenans" to distinguish this novel family of compounds from the allegedly carotenoid-derived sporopollenins.

In sharp contrast to the above studies, Py–GC/MS of the R3 yielded *n*-hydrocarbon products which are strongly attenuated with increasing carbon number. Even the use of mass chromatography to monitor characteristic ions for these compounds (*m/z* 55, 57 etc.) did not permit detection of homologous series beyond C_{10}. To confirm the low abundance of polymethylenic components in our dinoflagellate resting cyst cell wall material, we performed Py–GC/MS analysis of R3 at a higher Curie-point temperature (770°C) and for extended pyrolysis intervals (up to 5 s). These conditions, designed to expose the most refractory aliphatic networks, yielded no meaningful changes in the overall TIC profile. From this we conclude that the resistant biomacromolecule(s) in *L. polyedrum* resting cyst walls show(s) substantial structural differences relative to the algaenans described to date; instead this finding suggests that the recalcitrance of the resting cyst wall is due to chemical structures other than the aliphatic biopolymers encountered in the above species. The only reports of truncated *n*-hydrocarbon distributions are those describing pyrolysis products of kerogens rich in the fossilized remains of *Gloeocapsomorpha prisca* — a primitive unicellular organism that was prevalent during the Ordovician (e.g. Douglas *et al.*, 1991). Nevertheless, *n*-hydrocarbon products in pyrolyzates from this organism extend to C_{20}, well beyond those of *L. polyedrum*.

The only published report on algal cell wall composition that approaches what we have observed for *L. polyedrum* resting cysts is that of Derenne *et al.* (1996) who noted the "pronounced aromatic nature" of cell walls isolated from the marine chlorophyte *Chlorella marina*. The spectra yielded by both solid state ^{13}C NMR and IR analyses of *C. marina* cell walls showed features indicative of an aromatic composition and pyrolysis of the wall material liberated a complex mixture of products, dominated by aromatic and polyaromatic hydrocarbons. Major series, identified using mass chromatography of characteristic ions, included alkylbenzenes, alkylmethylbenzenes, alkyldimethylbenzenes, alkylnaphthalenes, and others. In all illustrated mass chromatograms, however, these series are comprised chiefly of aromatic moieties bearing alkyl side chains ranging from C_9–C_{19}, suggesting that long, saturated hydrocarbon chains do, in fact, form a significant part of the parent macromolecule. Again, therefore, these data contrast with the lack of extended side chains in the pyrolysate of *L. polyedrum* resting cyst cell wall material.

In the present investigation, alkaline CuO oxidation was employed to allow comparison of products yielded by chemical degradation to those obtained by thermal degradation (i.e., pyrolysis). CuO oxidation is a mild oxidative technique that proves especially useful in the analysis of ether and ester linked polyphenolic macromolecules. Although not previously rigorously applied to algal-derived resistant materials, CuO chemolysis has been used extensively to characterize recalcitrant biopolymers such as lignin and cutin which are synthesized by higher plants (e.g., Goñi and Hedges, 1990a,b, 1992, 1993; Goñi *et al.*, 1993).

As described above, oxygenated aromatic compounds are among the most common products yielded by CuO oxidation of our *L. polyedrum* cyst wall residue. It is especially noteworthy that methoxylated phenols, characteristic CuO oxidation products of lignins, are insignificant suggesting that cyst wall material is not related to woody tissues. The abundance of carboxylated phenols, however, is reminiscent of data obtained for fossil seed coats

(van Bergen *et al.*, 1994b), and may indicate a similar highly cross-linked polyphenolic structure. On the other hand, peaks representing C_{10} and C_{11} hydroxylated fatty acids suggest the presence of some aliphatic or lipid-like components in the cyst wall biomacromolecule. Furthermore, some carbohydrate may also be present as indicated by the C_4 di-acid, a feature consistent with results obtained from elemental analysis and Py–GC/MS.

It is difficult to account for our analytical results of *L. polyedrum* resting cyst walls by invoking sporopollenin substances built exclusively of carotenoid precursors. Two studies of synthetic sporopollenin (prepared by polymerization of carotenoids) have shown that phenolic compounds are released only in negligible amounts during potash-fusion, nitrobenzene oxidation, and AlI_3 degradation (Herminghaus *et al.*, 1988; Wehling *et al.*, 1989). In contrast, significant amounts of phenolic compounds were detected in the same studies when these techniques were applied to *Pinus* and *Corylus* sporopollenins. Similarly, in the present investigation, the type and amount of phenolic and other aromatic moieties resulting from pyrolytic and chemolytic analyses of dinoflagellate materials are inconsistent with the "traditional" carotenoid-based sporopollenin structure.

That these substances might be different is not a new idea; however, most of the previous comparisons of this nature are based on indirect observations and stem from the study of dinoflagellate, pollen, and spore cell walls recovered from the fossil record. Chaloner and Orbell (1971) found that dinoflagellate resting cysts showed a different behavior than pollen and spores when mixed fossil assemblages were centrifuged in a density gradient. Data presented by Correia (1971) suggested that, when exposed to increasing temperatures, pollen and spores show color changes at different rates than dinoflagellates and acritarchs. Sarjeant (1986) has commented that fossil dinoflagellates show a consistently different response to various stains when compared with fossil pollen. Finally, in studies of the preservation of organic matter within turbidite depositional sequences (Keil *et al.*, 1994; Cowie *et al.*, 1995), it was observed that dinoflagellate resting cysts tended to be preferentially preserved in horizons where oxidation had completely degraded pollen grains (Cowie and Keil, pers. comm.).

The apparent presence of a largely aromatic biomacromolecular substance in the resting cyst walls produced by a common marine dinoflagellate adds to our current understanding of the nature and distribution of highly resistant cell wall materials among the algae. A rapidly growing body of recent literature (reviewed in de Leeuw and Largeau, 1993) has reported that geologically preservable cell wall biopolymers from microalgal sources are highly aliphatic. These investigations, however, focus almost exclusively on species within the Chlorophyceae (green algae) and appear to involve only the cell walls enclosing vegetative stages. In contrast, materials investigated in the present study come from an unrelated algal division (the Dinoflagellata) and have been isolated from highly specialized reproductive cells, the hypnozygotic resting cysts. The function of the resting cyst walls differs markedly from the chlorophyte and eustigmatophyte cell walls studied previously. This functional difference is also reflected in the relatively thick and morphologically and structurally complex cell walls typical of many dinoflagellate resting cysts. Interestingly, cell coverings showing the closest chemical relationship to *L. polyedrum* resting cyst walls are those enclosing other reproductive propagules. Pollen exines, for example, may also be significantly aromatic in structure (Schultze Osthoff and Weirmann, 1987; Herminghaus *et al.*, 1988; Wehling *et al.*, 1989; Goñi *et al.*, 1995), and the fossil seed coats mentioned above appear to share both the polyphenolic and tocopherol signatures associated with our dinoflagellate material. This study thus represents one of the first reports of microalgal biomacromolecules having an aromatic character comparable to such substances produced by higher plants. Equally significant, however, is the almost complete absence of a network polymer comprised of extended aliphatic chains.

As with other highly refractory organic materials, it is still not yet possible to define the precise structure of the resistant biomacromolecule(s) in the *L. polyedrum* resting cyst cell wall, in spite of the availability of increasingly sophisticated analytical techniques. The same chemical and physical resilience responsible for the high preservation potential of these materials precludes complete analytical dissociation by currently known methods. This fact, together with the limited amount of sample available for analysis, restricted the present study to only a qualitative examination. Nevertheless, by showing that *L. polyedrum* resting cyst wall material lacks both the aliphaticity of algaenans and the carotenoid or carotenoid ester origin of sporopollenins, our work has important implications regarding the nomenclature and classification of highly resistant biomacromolecules. On one hand, this study supports previous proposals (e.g., Sarjeant, 1986) for a separate terminology dedicated to the resistant material found in dinoflagellate resting cyst walls. It is noteworthy that steps in this direction have already been taken: the term "dinosporin", for example, has been recently adopted by Fensome *et al.* (1993) in their extensive suprageneric classification of modern and fossil dinoflagellates, and will likely find wide usage among dinoflagellate biologists and paleontologists, despite the lack of any connotation of specific composition or structure.

However, the paucity of rigorous data concerning the chemical nature of these compounds necessitates a cautious definition and application of terms. It is clear from previous work (e.g., Prahl *et al.*, 1985; Guilford *et al.*, 1988; Goñi *et al.*, 1995) that not all spore and pollen exines contain a carotenoid-derived "sporopollenin". Similarly, as shown in the present study, "algaenan" (*sensu stricto*, see Tegelaar *et al.*, 1989) does not apply to all nonhydrolyzable cell wall substances produced by the algae. Thus, the examination of resting cyst cell wall biomacromolecules produced by other dinoflagellate species seems warranted before engaging in chemical definitions of "dinosporin".

CONCLUSIONS

(1) Successive treatment of initial *L. polyedrum* culture materials by solvent extraction, saponification, and acid hydrolysis had the intended effect of sequentially and predictably removing characterizable biochemicals. Optical assessment of products from these procedures indicated that the final residue consisted almost entirely of isolated walls of resting cysts. Chemical analyses suggested that artifactual products constitute a relatively minor proportion of the final residue.

(2) Investigation of the resting cyst wall material using a wide variety of optical, spectroscopic, pyrolytic, and chemolytic techniques revealed that, unlike other algaenans, there was little indication of the presence of a network polymer comprised of extended aliphatic chains. One exception was the presence of prist-1-ene as a prominent pyrolysis product from the final residue. This observation, taken together with the abundance of tocopherols in the lipid fraction of the initial material, suggests that bound tocopherols may play an important structural role in the resting cyst wall. The majority of the residue appeared to be composed of a macromolecular substance(s) that is relatively condensed and predominantly aromatic in composition.

(3) No convincing evidence for a carotenoid-based structure was detected in our analyses, and we conclude that *L. polyedrum* resting cyst wall material is compositionally distinct from traditionally defined "sporopollenin". Moreover, the minor importance of polymethylenic products revealed by pyrolysis of the dinoflagellate material indicates a biomacromolecular substance apparently unrelated to the strongly aliphatic algaenans found among the green algae.

Associate Editor—**C. Lergeau.**

Acknowledgements—The authors wish to thank the following individuals for technical assistance: Robert Nelson (WHOI, elemental analysis), John Reffner and Norm Colthup (Spectra-Tech, Inc., FT-IR microspectroscopy), Jos Pureveen (FOM, DT–MS), Carl Johnson (WHOI, Py–GC/MS), and John Hedges (University of Washington, CuO oxidation). Martin Head (University of Toronto) kindly supplied the photograph of fossil *Lingulodinium*. S. Derenne and J. W. de Leeuw are thanked for insightful reviews of an earlier version of this manuscript. This work was supported by a WHOI graduate research fellowship funded through the Amoco Foundation, Inc., National Science Foundation grants OCE-9001189, OCE-9300890, and OCE-8911226, the WHOI Ocean Ventures Fund, and a Phycological Society of America Grant-in-Aid of Research. Contribution 9345 of the Woods Hole Oceanographic Institution.

REFERENCES

Allard, B., Templier, J. and Largeau, C. (1997) Artifactual origin of mycobacterial bacteran. Formation of melanoidin-like artifactual macromolecular material during the usual isolation process. *Org. Geochem.* 21, in press.

Atkinson, A. W. Jr., Gunning, B. E. S. and John, P. C. L. (1972) Sporopollenin in the cell wall of *Chlorella* and other algae: Ultrastructure, chemistry, and incorporation of ^{14}C acetate, studied in synchronous cultures. *Planta* **107,** 1–32.

Barss, M. S. and Williams, G. L. (1973) Palynology and nannofossil processing techniques. *Geol. Surv. Can. Pap.* **73-26,** 1–25.

Berkaloff, C., Casadevall, E., Largeau, C., Metzger, P., Peracca, S. and Virlet, J. (1983) The resistant polymer of the walls of the hydrocarbon-rich alga *Botryococcus braunii*. *Phytochemistry* **22,** 389–397.

Bibby, B. T. and Dodge, J. D. (1972) The encystment of a freshwater dinoflagellate: a light and electron microscopical study. *Br. Phycol. J.* **7,** 85–100.

Boon, J. J. (1992) Analytical pyrolysis mass spectroscopy: new vistas opened by temperature-resolved in-source PYMS. *Int. J. Mass Spectrom. Ion Process.* **118/119,** 755–787.

Brunner, U. and Honegger, R. (1985) Chemical and ultrastructural studies on the distribution of sporopollenin-like biopolymers in six genera of lichen phycobionts. *Can. J. Bot.* **63,** 2221–2230.

Bujak, J. P. and Davies, E. H. (1983) *Modern and Fossil Peridiniineae*. AASP Contribution Series Number 13, 203 p. American Association of Stratigraphic Palynologists Foundation.

Burczyk, J. (1987a) Biogenetic relationships between ketocarotenoids and sporopollenins in green algae. *Phytochemistry* **26,** 113–119.

Burczyk, J. (1987b) Cell wall carotenoids in green algae which form sporopollenins. *Phytochemistry* **26,** 121–128.

Burczyk, J. and Dworzanski, J. (1988) Comparison of sporopollenin-like algal resistant polymer from cell wall of *Botryococcus. Scenedesmus* and *Lycopodium clavatum* by GC–pyrolysis.. *Phytochemistry* **27,** 2151–2153.

Burton, G. W. and Ingold, K. U. (1986) Vitamin E: Application of the principles of physical organic chemistry to the exploration of its structure and function. *Acc. Chem. Res.* **19,** 194–201.

Chaloner, W. G. and Orbell, G. (1971) A palaeobiological definition of sporopollenin. In *Sporopollenin*, ed. J. Brooks, P. R. Grant, M. Muir, P. van Gijzel and G. Shaw, p. 273–294. Proceedings of a symposium held at the Geology Department, Imperial College, London, 23–25 September, 1970, Academic Press, London.

Correia, M. (1971) Diagenesis of sporopollenin and other comparable organic substances: Application to hydrocarbon research. In *Sporopollenin*, ed. J. Brooks, P. R. Grant, M. Muir, P. van Gijzel and G. Shaw, p. 569–

620. Proceedings of a symposium held at the Geology Department, Imperial College, London, 23–25 September, 1970, Academic Press, London.

Cowie, G. L., Hedges, J. I., Prahl, F. G. and de Lange, G. J. (1995) Elemental and major biochemical changes across an oxidation front in a relict turbidite: An oxygen effect. *Geochim. Cosmochim. Acta* **59,** 33–46.

de Leeuw, J. W. and Largeau, C. (1993) A review of macromolecular organic compounds that comprise living organisms and their role in kerogen, coal, and petroleum formation. In *Organic Geochemistry*, ed. M. H. Engel and S. A. Macko, pp. 23–72. Plenum Press, New York.

de Leeuw, J. W., Baas, M., Brinkhuis, H., and Sinninghe Damsté, J. S. (1993). *Cyst cell wall biomacromolecules and dinosterol derivatives: molecular fossils of dinoflagellates.* 5th International Conference on Modern and Fossil Dinoflagellates, Zeist, the Netherlands, April 18–24, 1993, Abstract, pp. 28–29.

Delwiche, C. F., Graham, L. E. and Thomson, N. (1989) Lignin-like compounds and sporopollenin in *Coleochaete*, an algal model for land plant ancestry. *Science* **245,** 399–401.

Derenne, S., Largeau, C., Casadevall, E. and Berkaloff, C. (1989) Occurrence of a resistant biopolymer in the *L* race of *Botryococcus braunii. Phytochemistry* **28,** 1137–1142.

Derenne, S., Largeau, C., Casadevall, E. and Sellier, N. (1990) Direct relationship between the resistant biopolymer and the tetraterpenic hydrocarbon in the lycopadiene race of *Botryococcus braunii. Phytochemistry* **29,** 2187–2192.

Derenne, S., Largeau, C., Casadevall, E., Berkaloff, C. and Rousseau, B. (1991) Chemical evidence of kerogen formation in source rocks and oil shales via selective preservation of thin resistant outer walls of microalgae: Origin of ultralaminae. *Geochim. Cosmochim. Acta* **55,** 1041–1050.

Derenne, S., Largeau, C., Berkaloff, C., Rousseau, B., Wilhelm, C. and Hatcher, P. G. (1992) Non-hydrolysable macromolecular constituents from outer walls of *Chlorella fusca* and *Nanochlorum eucaryotum. Phytochemistry* **31,** 1923–1929.

Derenne, S., Largeau, C. and Berkaloff, C. (1996) First example of an algaenan yielding an aromatic-rich pyrolysate. Possible geochemical implications on marine kerogen formation. *Org. Geochem.* **24,** 617–627.

de Vries, P. J. R., Simons, J. and van Beem, A. P. (1983) Sporopollenin in the spore wall of *Spirogyra* (Zygnemataceae Chlorophyceae). *Acta Bot. Neerl.* **32,** 25–28.

Douglas, A. G., Sinninghe Damste, J. S., Fowler, M. G., Eglinton, T. I. and de Leeuw, J. W. (1991) Unique distributions of hydrocarbons and sulfur compounds released by flash pyrolysis from the fossilised alga *Gloeocapsomorpha prisca*, a major constituent in one of four Ordovician kerogens. *Geochimica Cosmochimica Acta* **55,** 275–291.

Eglinton, T. I., Boon, J. J., Minor, E. C. and Olson, R. J. (1996) Microscale characterization of algal and related particulate organic matter by direct temperature-resolved mass spectrometry. *Mar. Chem.* **52,** 27–54.

Eisenack, A. (1963) Hystrichosphären. *Bio. Rev. Cambridge Philos. Soc.* **38,** 107–139.

Erdtman, G. (1961) The acetolysis method. A revised description. *Sven. Bot. Tidskr.* **54,** 561–564.

Evitt, W. R. (1961) Observations on the morphology of fossil dinoflagellates. *Micropaleontology* **7,** 385–420.

Evitt, W. R. (1985) *Sporopollenin Dinoflagellate Cysts: Their Morphology and Interpretation*, 333 p. American Association of Stratigraphic Palynologists Foundation.

Fensome, R. A., Taylor, F. J. R., Norris, G., Sarjeant, W. A. S., Wharton, D. I. and Williams, G. L. (1993) *A Classification of Living and Fossil Dinoflagellates.* Micropaleontology, Special Publication Number 7, 351 p. Sheridan Press, Hanover, PA.

Flaviano, C., Le Berre, F., Derenne, S., Largeau, C. and Connan, J. (1994) First indications of the formation of kerogen amorphous fractions by selective preservation. Role of non-hydrolysable macromolecular constituents of Eubacterial cell walls. *Org. Geochem.* **22,** 759–771.

Fritz, L., Anderson, D. M. and Triemer, R. E. (1989) Ultrastructural aspects of sexual reproduction in the red tide dinoflagellate *Gonyaulax tamarensis. J. Phycol.* **25,** 95–107.

Gelin, F., Boogers, I., Noordeloos, A. A. M., Hatcher, P. G., Sinninghe Damste, J. S. and de Leeuw, J. W. (1996) Novel, resistant microalgal polyethers: An important sink of organic carbon in marine environments? *Geochim. Cosmochim. Acta* **60,** 1275–1280.

Geisert, M., Rose, T., Bauer, W. and Zahn, R. K. (1987) Occurrence of carotenoids and sporopollenin in *Nanochlorum eucaryotum* a novel marine alga with unusual characteristics. *BioSystems* **20,** 133–142.

Goñi, M. A. and Hedges, J. I. (1990a) Cutin-derived CuO reaction products from purified cuticles and tree leaves. *Geochim. Cosmochim. Acta* **54,** 3065–3072.

Goñi, M. A. and Hedges, J. I. (1990b) The diagenetic behavior of cutin acids in buried conifer needles and sediments from a coastal marine environment. *Geochim. Cosmochim. Acta* **54,** 3083–3093.

Goñi, M. A. and Hedges, J. I. (1992) Lignin dimers: Structures, distribution, and potential geochemical applications. *Geochim. Cosmochim. Acta* **56,** 4025–4043.

Goñi, M. A. and Hedges, J. I. (1993) Molecular-level characterization of marine-derived sedimentary organic matter by alkaline CuO oxidation: sources and reactivities of organic matter from Skan Bay (Alaska) sediments. *Chem. Geol.* **107,** 483–485.

Goñi, M. A., Nelson, B., Blanchette, R. A. and Hedges, J. I. (1993) Fungal degradation of wood lignins: Geochemical perspectives from CuO-derived phenolic dimers and monomers. *Geochim. Cosmochim. Acta* **57,** 3985–4002.

Goñi, M. A., Kokinos, J. P., Hatcher, P. and Eglinton, T. I. (1995) Chemical, pyrolytic and spectroscopic characterization of resistant biopolymer(s) present in pollen. In *Organic Geochemistry: Developments and Applications to Energy, Climate, Environment and Human History*, ed. J. O. Grimalt and C. Dorronsoro, pp. 983–985. Selected papers from the 17th International Meeting on Organic Geochemistry, 4th–8th September 1995, Donostia–San Sebastián, The Basque Country, Spain, A.I.G.O.A.

Goñi, M. A., Kokinos, J. P., Hatcher, P., Boon, J. J., Martoglio, A. and Eglinton, T. I. (1998) *Chemical, pyrolytic and spectroscopic characterization of resistant biopolymers present in pollen*, in preparation.

Good, B. H. and Chapman, R. L. (1978) The ultrastructure of *Phycopeltis* (Chroolepidaceae: Chlorophyta). I. Sporopollenin in the cell walls. *Am. J. Bot.* **65,** 27–33.

Goodman D. K. (1987) Dinoflagellate cysts in ancient and modern sediments. In *The Biology of Dinoflagellates*, ed. F. J. R. Taylor, Vol. 21, pp. 649–722. Botanical Monographs, Blackwell Scientific Publishers, Oxford.

Goossens, H., de Leeuw, J. W., Schenck, P. A. and Brassell, S. C. (1984) Tocopherols as likely precursors of pristane in ancient sediments and crude oils. *Nature* **312,** 440–442.

Goth, K., de Leeuw, J. W., Püttmann, W. and Tegelaar, E. W. (1988) Origin of messel oil shale kerogen. *Nature* **339,** 759–761.

Gray, J. (1965) Techniques in palynology; Part III. In *Handbook of Paleontological Techniques*, ed. B. Kummel

and D. M. Raup, pp. 469–706. Freeman and Company, San Francisco.

Guilford, W. J., Schneider, D. M., Labovitz, J. and Opella, S. J. (1988) High resolution solid state ^{13}C NMR spectroscopy of sporopollenins from different plant taxa. *Plant Physiol.* **86,** 134–136.

Hedges, J. I. and Ertel, J. R. (1982) Characterization of lignin by capillary gas chromatography of cupric oxide oxidation products. *Anal. Chem.* **54,** 174–178.

Herminghaus, S., Gubatz, S., Arendt, S. and Wiermann, R. (1988) The occurrence of phenols as degradation products of natural sporopollenin — a comparison with "synthetic sporopollenin". *Z. Naturforsch.* **43c,** 491–500.

Jux, U. (1971) Über den feinbau der wandungen einiger Tertiärer dinophyceen–zysten und achritarcha *Hystichosphaeridium, Impletosphaeridium, Lingulodinium. Palaeontographica, Abt. B* **132,** 165–174.

Kadouri, A., Derenne, S., Largeau, C., Casadevall, E. and Berkaloff, C. (1988) Resistant biopolymer in the outer walls of *Botryococcus braunii, B* race. *Phytochemistry* **27,** 551–557.

Keil, R. G., Hu, F. S., Tsamakis, E. and Hedges, J. I. (1994) Pollen grains deposited in marine sediments are degraded only under oxic conditions. *Nature* **369,** 639–641.

Kokinos, J. P. (1994) Studies on the cell wall of dinoflagellate resting cysts: Morphological development, ultrastructure, and chemical composition. Ph. D. Thesis, Massachusetts Institute of Technology/Woods Hole Oceanographic Institution, Technical Report WHOI-94-10, 234 p.

Kokinos, J. P. and Anderson, D. M. (1995) Morphological development of resting cysts in cultures of the marine dinoflagellate *Lingulodinium polyedrum* (= *L. machaerophorum*). *Palynology* **19,** 143–166.

König, J. and Peveling, E. (1980) Vorkommen von sporopollenin in der zellwand des phycobionten Trebouxia. (Sporopollenin in the cell wall of the phycobiont *Trebouxia*). *Z. Pflanzenphysiol. (Int. J. Plant Physiol.)* **98,** 459–464.

Largeau, C., Casadevall, E., Kadouri, A. and Metzger, P. (1984) Formation of Botryococcus-derived kerogens — Comparative study of immature torbanites and of the extant alga *Botryococcus braunii. Org. Geochem.* **6,** 327–332.

Largeau, C., Derenne, S., Casadevall, E., Kadouri, A. and Sellier, N. (1986) Pyrolysis of immature Torbanite and of the resistant biopolymer (PRB A) isolated from the extant alga *Botryococcus braunii.* Mechanism of formation and structure of Torbanite. *Org. Geochem.* **10,** 1023–1032.

Larter, S. R., Solli, H., Douglas, A. G., De Lange, F. and de Leeuw, J. W. (1979) The occurrence and significance of prist-1-ene in kerogen pyrolysates. *Nature* **279,** 405–408.

Larter, S. R., Solli, H. and Douglas, A. G. (1981) Phytol-containing melanoidins and their bearing on the fate of isoprenoid structures in sediments. In *Advances in Organic Geochemistry*, ed. M. Bjorøy *et al.*), pp. 513–523. Proceedings of the 10th International Meeting on Organic Geochemistry, University of Bergen, Norway, 14–18 September 1981.

Larter, S. R. and Horsfield, B. (1993) Determination of structural components of kerogens by the use of analytical pyrolysis methods. In *Organic Geochemistry*, ed. M. H. Engel and S. A. Macko, pp. 271–287. Plenum Press, New York.

Li, M., Larter, S. R., Taylor, P., Jones, D. M., Bowler, B. and Bjorøy, M. (1995) Biomarkers or not biomarkers? A new hypothesis for the origin of pristane involving derivation from methyltrimethyltridecylchromans (MTTCs) formed during diagenesis from chlorophyll and alkylphenols *Org. Geochem.* **23,** 159–167.

Morrill, L. C. and Loeblich, A. R. III (1981) The dinoflagellate pellicular wall layer and its occurrence in the division Pyrrhophyta. *J. Phycol.* **17,** 315–323.

Mulder, M. M., van der Hage, E. R. E. and Boon, J. J. (1992) Analytical in source pyrolytic methylation electron impact mass spectrometry of phenolic acids in biological matrices. *Phytochem. Anal.* **3,** 165–172.

Pfiester, L. A. (1984) Sexual reproduction. In *Dinoflagellates*, ed. D. L. Spector, pp. 181–199. Academic Press, Orlando, FL.

Pfiester, L. A. (1989) Dinoflagellate sexuality. *Int. Rev. Cytol.* **114,** 249–272.

Pfiester, L. A. and Anderson, D. M. (1987) Dinoflagellate Reproduction. In *The Biology of Dinoflagellates*, ed. F. J. R. Taylor, Vol. 21, pp. 611–648. Botanical Monographs, Blackwell Scientific Publishers, Oxford.

Prahl, A. K., Springstubbe, H., Grumbach, K. and Wiermann, R. (1985) Studies on sporopollenin biosynthesis: The effect of inhibitors of carotenoid biosynthesis on sporopollenin accumulation. *Z. Naturforsch.* **40c,** 621–626.

Puel, F., Largeau, C. and Giraud, G. (1987) Occurrence of a resistant biopolymer in the outer walls of the parasitic alga *Prototheca wickerhamii* (Chlorococcales): Ultrastructure and chemical studies. *J. Phycol.* **23,** 649–656.

Rouxhet, P. G., Robin, P. L. and Nicaise, G. (1980) Characterization of kerogens and of their evolution by infrared spectroscopy. In *Kerogen: Insoluble Organic Matter from Sedimentary Rocks*, ed. B. Durand, pp. 163–190. Éditions Technip, Paris.

Sarjeant, W. A. S. (1986) Review of Evitt, W. R., 1985, Sporopollenin Dinoflagellate Cysts: Their Morphology and Interpretation. *Micropaleontology* **32,** 282–285.

Schmitter, R. E. (1971) The fine structure of *Gonyaulax polyedra*, a bioluminescent marine dinoflagellate. *J. Cell Sci.* **9,** 147–173.

Schmitter R. E. (1989) Structure and function of globular bodies in dinoflagellate cells [Abstract]. *Fourth International Conference on Modern and Fossil Dinoflagellates*, p. 92, Marine Biological Laboratory, Woods Hole, Massachusetts, Program and Abstracts.

Schultze Osthoff, K. and Weirmann, R. (1987) Phenols as integrated compounds of sporopollenin from *Pinus* pollen. *J. Plant Physiol.* **131,** 5–15.

Shaw, G. and Yeadon, A. (1966) Chemical studies on the constitution of some pollen and spore membranes. *J. Chem. Soc. C* **1,** 16–22.

Spector, D. L. (Ed.) (1984) *Dinoflagellates*, 545 p., Academic Press, Orlando, FL.

Tappan, H. (1980) *The Paleobiology of Plant Protists*, 1028 p. W. H. Freeman and Company, San Francisco.

Taylor, D. L. (1968) *In situ* studies on the cytochemistry and ultrastructure of a symbiotic marine dinoflagellate. *J. Mar. Biol. Assoc. U.K.* **48,** 349–366.

Taylor, F. J. R. (Ed.) (1987) *The Biology of Dinoflagellates.* Botanical Monographs, Vol. 21, 785 p. Blackwell Scientific Publications, Oxford.

Tegelaar, E. W., de Leeuw, J. W., Derenne, S. and Largeau, C. (1989) A reappraisal of kerogen formation. *Geochim. Cosmochim. Acta* **53,** 3103–3106.

Tegelaar, E. W. (1990) Resistant biomacromolecules in morphologically characterized constituents of kerogen: A key to the relationship between biomass and fossil fuels. Ph.D. thesis, Rijksuniversiteit Utrecht.

van Bergen, P. F., Collinson, M. E., Sinninghe Damsté, J. S. and de Leeuw, J. W. (1994a) Chemical and microscopical characterization of inner seed coats of fossil water plants. *Geochim. Cosmochim. Acta* **58,** 231–239.

van Bergen, P. F., Goñi, M., Collinson, M. E., Barrie, P. J., Sinninghe Damsté, J. S. and de Leeuw, J. W. (1994b) Chemical and microscopic characterization of outer seed coats of fossil and extant water plants. *Geochim. Cosmochim. Acta* **58,** 3823–3844.

Walker, L. M. (1984) Life histories, dispersal, and survival in marine, planktonic dinoflagellates. In *Marine Plankton Life Cycle Strategies*, ed. K. A. Steidinger and L. M. Walker, p. 19–34. CRC Press, Boca Raton, FL.

Wehling, K., Niester, C., Boon, J. J., Willemse, M. T. M. and Wiermann, R. (1989) *p*-Coumaric acid — a monomer in the sporopollenin skeleton. *Planta* **179,** 376–380.

Williams, G. L. and Bujak, J. P. (1985) Mesozoic and Cenozoic dinoflagellates. In *Plankton Stratigraphy*, ed. H. M. Bolli, J. B. Saunders and K. Perch-Nielsen, pp. 847–964. Cambridge Earth Science Series, Cambridge University Press, Cambridge.

Williams, G. L., Stover, L. E. and Kidson, E. J. (1993) Morphology and stratigraphic ranges of selected Mesozoic–Cenozoic dinoflagellate taxa in the northern hemisphere. *Geol. Surv. Can. Pap.* **92-10,** 1–137.

Zetsche, F., Kalt, P., Leichti, J. and Ziegler, E. (1937) Zur konstitution des lycopodiumsporinins des tasmins und des lange-sporonins. *J. Prakt. Chem.* **148,** 67–84.

Zetsche, F. and Vicari, H. (1931) Untersuchungen über die membran der sporen und pollen. *Helv. Chim. Acta* **14,** 58–78.